

Inverse magnetocaloric effect and phase separation induced by giant van Hove singularity in itinerant ferromagnetic metal

P. A. Igoshev^{1,2} and I. A. Nekrasov³

¹*M. N. Mikheev Institute of Metal Physics, 620041,
S. Kovalevskoj Str. 19, Ekaterinburg, Russia*

²*Amirkhanov Institute of Physics of DFRC of RAS, Makhachkala 367003, Russia*

³*Institute of Electrophysics UB RAS, 620016,
Amundsena Str. 106, Ekaterinburg, Russia*

Abstract

Magnetic phase separation and magnetocaloric effect is considered within the Hubbard model for face-centered cubic (fcc) lattice with giant van Hove singularity of electron spectrum at band bottom. Within the Hartree-Fock approximation it is shown that such model of itinerant magnet exhibits the first-order ferromagnet-paramagnet phase transition (FOPT) with phase separation and inverse magnetocaloric effect deep inside the phase separation region. The thermodynamic theory based on Landau expansion for grand potential for the ferromagnetic-paramagnetic phase transition is developed for phase-separated state. It is rigorously shown that ferromagnetic phase involved in the phase separated state exhibits negative magnetic susceptibility in the vicinity of tricritical point. Thus, an entropy of the magnetically ordered phase may increase when the magnetic field is applied which implies inverse character of the total magnetic entropy change ΔS . Temperature dependence of ΔS for the mean-field solution of the non-degenerate Hubbard model is analyzed in detail for different band filling values. The possibility to control ΔS sign by changing both the temperature and the band filling of magnetocaloric materials is demonstrated and this seems to be promising from the point of view of interpretation a lot of experimental data and possible technological applications. It is shown that giant van Hove singularity, being a main cause of phase separation, strongly affects temperature dependence of ΔS in the vicinity of tricritical point.

PACS numbers:

I. INTRODUCTION

The magnetocaloric effect (MCE), i.e. a change of a sample temperature T (entropy S) when the external magnetic field is applied under the condition of fixed entropy (temperature), is observed in a lot of magnetically ordered systems. The strength of MCE typically has maximal value close to critical temperature of magnetic phase transition. Over the past 40 years, a huge amount of experimental data on MCE has been accumulated, see reviews 1–3. The current state of affairs in the field of materials used for magnetic cooling is described in Ref. 4, whereas medical applications are reviewed in Ref. 5. Details of standard theoretical approaches to the study of MCE are described in the review 6.

The temperature profile of isothermal entropy change $\Delta S(T)$ and its maximum absolute value ΔS_{\max} substantially depend on the order of magnetic phase transition as well as on the nature of the electronic states forming magnetic order. Most important quantity for applications characterizing the magnetic cooling efficiency is *relative cooling power* (RCP) proportional to ΔS_{\max} , and its peak width. Thus, an ability to calculate $\Delta S(T)$ profile for real materials based on characteristics of their electronic structure is of a great importance for practical applications. In addition, not only a large value ΔS at peak temperature, but also the table-like temperature dependence of ΔS can be used to construct an ideal Ericsson cycle of magnetic refrigeration. Recently the compounds exhibiting such behaviour attracted a lot of attention^{7–11}.

Perhaps the most known material being examined for practical use is rare-earth system $\text{Gd}_5\text{Si}_2\text{Ge}_2$ exhibiting so-called giant MCE ($\Delta S_{\max} \sim 19$ J/kg/K under the magnetic field 5 T) at room temperature¹². The magnetic properties of this system are mainly driven by localized magnetic moments of Gd f -shell. For this compound, the position of $\Delta S(T)$ maximum is close to the Curie temperature $T_C \sim 273$ K of the first-order ferromagnetic (FM)–paramagnetic (PM) magnetic phase transition.

Rare-earth compounds are not only materials with remarkable MCE properties. There are some examples of transition metal compounds which also exhibit large and unexplained MCE potential values. The MnAs , $\text{MnFeP}_{0.45}\text{As}_{0.55}$ and $\text{La}(\text{Fe}_x\text{S}_{1-x})_{13}$ systems demonstrate ΔS_{\max} value close to that of the $\text{Gd}_5\text{Si}_2\text{Ge}_2$ system. Note that, first-order FM-PM phase transition in the following compounds occurs at temperature close to room temperature: 318 K in MnAs ¹³, about 300 K in $\text{MnFeP}_{0.45}\text{As}_{0.55}$ ¹⁴. First-order FM-PM phase transition

occurs about 195 K in $\text{La}(\text{Fe}_{0.88}\text{Si}_{0.12})_{13}$ and its origin is likely the peak of electron density of states in the vicinity of Fermi level in paramagnetic phase¹⁵. Interestingly, the order of FM–PM magnetic phase transition in the system $\text{La}(\text{Fe}_x\text{Si}_{1-x})_{13}$ depends on the concentration of Si: at low concentrations there is a first-order phase transition (FOPT), while at larger concentrations – second-order phase transition (SOPT) occurs¹⁶. Magnetism in the systems $\text{MnFeP}_{0.45}\text{As}_{0.55}$ and $\text{La}(\text{Fe}_x\text{Si}_{1-x})_{13}$ has pronounced itinerant character¹⁷.

All above mentioned compounds demonstrate so called *direct* MCE: an increase of the magnetic field within an isothermal process results in the entropy decrease ($\Delta S < 0$), and the temperature increase within the adiabatic process ($\Delta T > 0$). However, there is another class of compounds exhibiting opposite response to an applied magnetic field ($\Delta T < 0$, $\Delta S > 0$), which is named *inverse* MCE.

Typical classes of systems with inverse MCE are Heusler alloys (*e.g.* NiMnIn ¹⁸, NiMnSn ¹⁹, $\text{Ni}_2\text{Mn}_{1-x}\text{Cu}_x\text{Ga}$ ²⁰ with martensitic antiferromagnetic (AFM)–FM phase transition), some manganites (*e.g.* $\text{Pr}_{0.5}\text{Sr}_{0.5}\text{MnO}_3$ ²¹, $\text{MnFeP}_{0.8}\text{Ge}_{0.2}$ ²² (with PM+FM phase separation), $\text{La}_{1-x}\text{Ca}_x\text{MnO}_3$ ²³), intermetallic compounds (*e.g.* PrNi_5 ²⁴, ErRu_2Si_2 ²⁵, $\text{CoMnSi}_{1-x}\text{Ge}_x$ ²⁶), for more details see the reviews^{1,2,6,27}. In the Heusler alloys, the FM–PM magnetic phase transitions typically give direct MCE while inverse MCE occurs under FM-AFM transition.

Besides observed above ordinary ferromagnetic systems, there are also systems where the ferromagnetic order coexists with some other ordered phases in terms of phase separation (PS): $\text{La}_{0.27}\text{Nd}_{0.40}\text{Ca}_{0.33}\text{MnO}_3$ ²⁸ (FM+charge-ordered phase separation), $\text{Mn}_{0.99}\text{Cu}_{0.01}\text{As}$, $\text{Gd}_5\text{Ge}_{2.3}\text{Si}_{1.7}$ ²⁹ (FM+AFM phase separation). The compound (alloy) FeRh exhibits large value of $\Delta S_{\text{max}} > 0$ (inverse MCE) under corresponding FM-AFM FOPT upon temperature decrease with critical temperature 270 K^{30,31}. This phase transition goes through FM+AFM phase separation region.

There are also some materials that exhibit inverse MCE: MnRhAs ³², Co and Mn Co-Doped Ni_2MnGa ²⁰, $\text{Er}_2\text{Fe}_{17}$ ^{33,34}, DyAl_2 ³⁵, $\text{Pr}_{0.46}\text{Sr}_{0.54}\text{MnO}_3$ ³⁶ in the vicinity of FOPT temperature. Typically, there are two different temperatures for inverse and direct MCE. Moreover, an inverse MCE provides an additional peak in ΔS temperature profile (see *e.g.* $\text{Eu}_{0.55}\text{Sr}_{0.45}\text{MnO}_3$ ²⁸, $\text{Ni}_{50}\text{Mn}_{33.13}\text{In}_{13.90}$ ¹⁸, ErGa_2 , HoGa_2 ³⁷, HoFeSi ³⁸).

Previously some theoretical studies of MCE in materials and corresponding models with FOPT were performed. A Monte-Carlo-based solution of the Potts-Blume-Emery-Griffiths model was used to investigate a series of $\text{Ni}_{45}\text{Co}_5\text{Mn}_{37}\text{In}_{13}$ ³⁹ and Ni-Co-Mn-(Sn,Al) alloys⁴⁰,

which have two phase transitions with direct and inverse MCE. Within the Potts-Blume-Emery-Griffiths model, the inhomogeneity arising during the FOPT was taken into account by introducing an additional term to the Hamiltonian responsible for a disorder, which simulates the mixing of martensitic and austenitic phases. Investigation of MCE in the case of SOPT for the mean-field treated Hubbard model for different bare densities of states was performed in Refs. 6,41. Theoretical study of MCE for FM-AFM FOPT including also ferrimagnetic states, taking into account the possibility of phase separated state formation within the Hubbard model was performed for Bethe⁴² and square⁴³ lattices.

Another direction of theoretical studies is based on phenomenological Landau theory. The latter was designed to describe the FM-PM SOPT using a simple free energy functional⁴⁴. However, this theory exhibits wide opportunities to consider more general cases, *e.g.* in the case of FOPT. The Landau theory equally well can be applied to both itinerant and localized electron systems. For the itinerant systems a direct derivation of Landau series coefficients within the Stoner approximation can be done straightforward starting from bare electronic density of states⁴⁵. However, the phenomenological approach (corresponding to paramagnon renormalization of Landau series coefficients) proved itself to be more successful⁴⁵⁻⁴⁸. Some examples of the Landau theory application for explanation of FOPT and MCE in itinerant systems $\text{Co}(\text{S,Se})_2$, $\text{Lu}(\text{Co,Al})_2$, and $\text{Lu}(\text{Co,Ga})_2$ can be found in Ref. 17. Necessary for FOPT sign changes of Landau series coefficients may be provided due to the presence of peculiarities of density of states in the vicinity of the Fermi level¹⁵ or due to an introduction of additional interactions (*e. g.* AB_2 compounds¹⁷, MnAs ^{6,49,50}, $\text{MnFeP}_{0.45}\text{As}_{0.55}$ ⁵¹, YCo_2 ^{52,53}).

However, phase separation accompanying FOPT in metal systems stays beyond this approach and is somehow unavailable without an appropriate extension of Landau theory.

Thus, there is a problem of theoretical modeling and explanation of MCE in itinerant systems exhibiting FOPT FM-PM. Another complexity comes from necessary presence of phase-separated state in itinerant systems near FOPT region, and pure localized electron model (without itinerant component) can not consistently treat appearing inhomogeneities^{50,54-59}. At the moment there is a lack of theoretical studies of MCE for variety of experimental data in systems with FOPT and PS. Additional issue is that conventional Maxwell relations for experimental data treatment in a case of FOPT should be applied with a great caution. One should also take into account that phase volumes of PS state depend on temperature and magnetic field²⁸. Neglecting this dependency leads to spurious results^{54,60}, which were

discussed in Refs. 39,61.

The plan of the presentation is the following. An extension of the Landau theory for an account of PS state during FM-PM FOPT is presented in Section II. Section III contains the example of MCE within the mean-field solution of the non-degenerate Hubbard model for an face-centered cubic lattice with the parameter set corresponding to the position of Fermi level in the vicinity of giant van Hove singularity of the electronic density of states. The paper is ended by concluding remarks in Sec. IV.

II. FM-PM FOPT THERMODYNAMICS: THE EXTENSION OF LANDAU THEORY

Conventional Landau functional (free energy) does not allow to describe phase separation which can accompany any FOPT in itinerant magnets^{62–64}. The Landau functional typically is considered as a functional of the magnetization only, and besides the latter plays a role of an order parameter. From a general point of view, in itinerant magnet order parameter jump at FOPT point should result in band filling jump which in turn may result in phase separation formation. Instead of introducing band filling n as an inner argument of free energy, chemical potential μ should be introduced as an argument of the Landau functional and grand potential Ω — instead of free energy F ^{44,65}. In this section we present general thermodynamical approach to FOPT including PS state as well as to standard SOPT within the Landau theory.

Let us write Landau expansion for grand potential Ω with respect to the order parameter m (the coefficients A_α^Ω depend on T and μ)

$$\Omega(T, \mu, h|m) = A_0^\Omega(T, \mu) + A_2^\Omega(T, \mu)m^2 + A_4^\Omega(T, \mu)m^4 + A_6^\Omega(T, \mu)m^6 - hm, \quad (1)$$

where $A_6^\Omega > 0$ to provide stable solution. The coefficients A_α^Ω up to sixth order are hold to supply not only SOPT but also the possibility of FOPT.

External arguments (*i.e.* set up by environment such as μ, T and h) are written before the vertical line ‘|’, internal argument, magnetization m , which can be found by minimization of Ω under given external parameters, is written after ‘|’. Note that the internal parameter specifies particular phase for the system. We consider phase transitions between phases differing by a value of m only, *e. g.* paramagnetic-ferromagnetic or antiferromagnetic-

ferrimagnetic phase transitions.

The *equation of state* defining magnetization $m = m(T, \mu, h)$ for given T, μ and h is determined by extremum condition of Eq. (1) $\partial\Omega/\partial m = 0$, and has a form

$$f(T, \mu|m) = h, \quad (2)$$

where

$$f(T, \mu|m) = 2(A_2^\Omega(T, \mu)m + 2A_4^\Omega(T, \mu)m^3 + 3A_6^\Omega(T, \mu)m^5) \quad (3)$$

and $\partial f/\partial m > 0$ (the criterion of Ω minimum at m point).

We are interested in the calculation of zero-field magnetic susceptibility

$$\left(\frac{dm}{dh}\right)_{h=0} = \left(\frac{\partial m}{\partial h}\right)_{h=0} + \eta_{\text{env}}(h=0) \left(\frac{\partial m}{\partial \mu}\right)_{h=0}, \quad (4)$$

where the derivative

$$\eta_{\text{env}} = d\mu/dh \quad (5)$$

originates from the dependence $\mu = \mu(h)$, which in turn should be setup to provide constraints determined by physical environment.

Using Eq. (2) we get μ -fixed (as denoted by bar) zero-field magnetic susceptibility $\bar{\chi} \equiv (\partial m/\partial h)_{h=0} = (\partial f/\partial m)_{h=0}^{-1}$, i. e.

$$\bar{\chi} = \frac{1}{2}(A_2^\Omega + 6A_4^\Omega m^2 + 15A_6^\Omega m^4)^{-1}, \quad (6)$$

where m satisfies Eq. (2) at $h = 0$. At $h = 0$ the Eq. (2) may have up to two solutions $m \geq 0$. While in the case $A_2^\Omega < 0$ unique minimum exists at arbitrary values of A_4^Ω and positive A_6^Ω , at $A_2^\Omega > 0$, $m = 0$ Ω minimum exists (corresponding to PM state) and in the case $(A_4^\Omega)^2 > 3A_2^\Omega A_6^\Omega$, $A_4^\Omega < 0$, additional finite- m minimum of Ω exists, $m = m_{\text{FM}}$,

$$m_{\text{FM}}^2 = \frac{-A_4^\Omega + \sqrt{(A_4^\Omega)^2 - 3A_2^\Omega A_6^\Omega}}{3A_6^\Omega}. \quad (7)$$

corresponding to FM state. Then the Eq. (7) can be written as

$$m_{\text{FM}}^2 = -\frac{2A_2^\Omega}{A_4^\Omega}. \quad (8)$$

For magnetically ordered phase, we calculate $\bar{\chi}$, taking into account Eqs. (2) and (6),

$$\bar{\chi}_{\text{FM}} = \frac{1}{8m_{\text{FM}}^2(A_4^\Omega + 3A_6^\Omega m_{\text{FM}}^2)}. \quad (9)$$

For PM solution $m = m_{\text{PM}} = 0$, from Eq. (6) we have

$$\bar{\chi}_{\text{PM}} = \frac{1}{2A_2^\Omega}. \quad (10)$$

Further we consider two different cases: (i) single-phase (homogeneous) and (ii) phase-separated state (see next subsection).

A. Magnetic susceptibility at fixed band filling

For a single-phase case (i) band filling defined as $n = -\partial\Omega/\partial\mu = \mathbf{n}(\mu, T|m)$, where

$$\mathbf{n}(T, \mu|m) = -(\dot{A}_0^\Omega + \dot{A}_2^\Omega m^2 + \dot{A}_4^\Omega m^4 + \dot{A}_6^\Omega m^6), \quad (11)$$

where $\dot{A}_\alpha^\Omega = \partial A_\alpha^\Omega/\partial\mu$. Therefore for the single-phase state there comes additional h -independent condition to determine μ

$$\mathbf{n}(T, \mu|m) = n \quad (12)$$

as a function of T and m . Magnetic field h affects the system only through m and μ .

The fixed band filling magnetic susceptibility (as denoted by lower index “ n ”) reads

$$\chi_n \equiv \left(\frac{dm}{dh} \right)_{n,h=0} \quad (13)$$

is obtained directly from Eq. (4), where μ changes consistently with m to satisfy Eq. (12), so that $\eta_n \equiv (d\mu/dh)_{n,h=0}$ and

$$\eta_n = - \left(\frac{\partial \mathbf{n}/\partial m}{\partial \mathbf{n}/\partial \mu} \right)_{h=0} \chi_n. \quad (14)$$

Therefore we get

$$\chi_n = \left(\frac{\partial f}{\partial m} - \frac{\partial f}{\partial \mu} \frac{\partial \mathbf{n}/\partial m}{\partial \mathbf{n}/\partial \mu} \right)^{-1} \quad (15)$$

which is always positive for any single-phase metallic electron system.

B. Magnetic susceptibility of phases for phase-separated state

Now we consider the case (ii) for phase-separated state caused by FOPT with PM and FM phases (instead of these phases there can be any other pair of phases differing from each

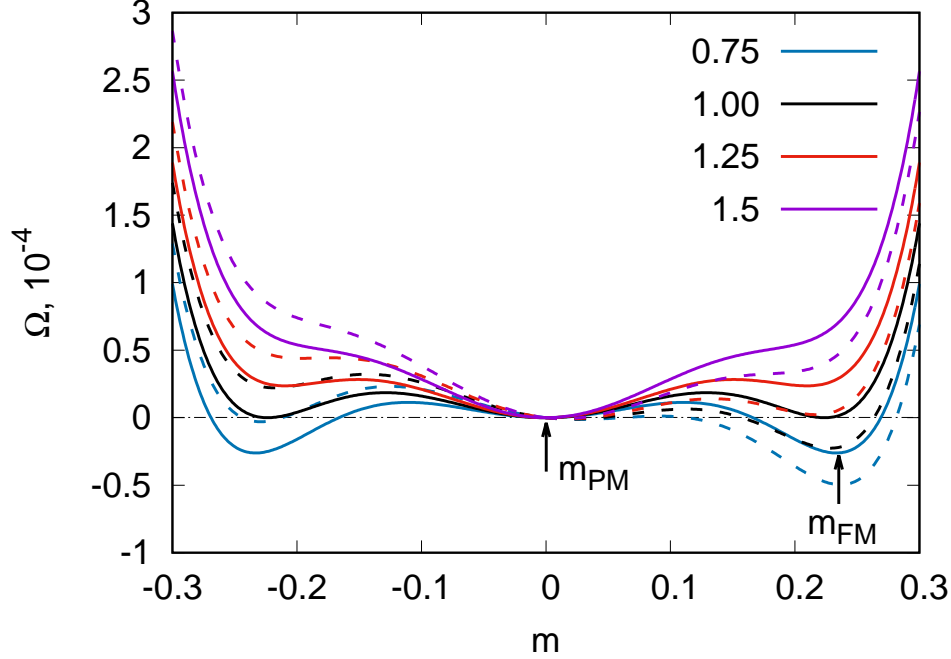


FIG. 1: Schematic plot of $\Omega(m)$ for $A_4^\Omega = -0.1$, $A_6^\Omega = 1$, and different values of A_2^Ω in units of $A_{2,\text{FOPT}}^\Omega$ (shown in legend). Arrows show the positions of minimum of $\Omega(m)$, corresponding to minimum position $m = m_{\text{FM}}(m_{\text{PM}})$ for FM (PM) phase. Solid (dashed) lines show the result at $h = 0$ ($h = 10^{-4}$).

other only by the presence of non-zero component of total magnetization). Main difference of FOPT in itinerant systems from the FOPT in localized systems is that in the former case, a jump of the order parameter m (magnetization) at the transition point leads to a band filling jump. For the phase-separated state total band filling is a weighted sum of both phase band fillings, see Eq. (11), satisfying Eq. (2) at the thermodynamic equilibrium. At given T and h at FOPT line the criterion of PS appearance is a falling of n into the band filling jump interval, see details in Refs. 42,63–65. Therefore all extensive quantities describing PS state acquire additional linear dependence on band filling n . Thus, for μ fixed at FOPT line band filling n plays a role of additional degree of freedom.

At FOPT line, grand potential $\Omega(\mu, T, h|m_\Phi)$ for different phases $\Phi = \text{FM}, \text{PM}$ involved in PS should be equal, where m_{FM} (FM phase) and m_{PM} (PM phase) are the roots of Eq. (2). The definition of phase separation boundary line $\mu = \mu_{\text{PS}}(T, h)$ reads

$$\Omega(T, \mu_{\text{PS}}(T, h), h|m_{\text{FM}}) = \Omega(T, \mu_{\text{PS}}(T, h), h|m_{\text{PM}}). \quad (16)$$

In the case of a zero magnetic field $h = 0$, Eq. (16) becomes $A_4 + 2A_6 m_{\text{FM}}^2 = 0$. Using

the Eq. (7) one can get zero-field FOPT line equation in terms of T and μ variables

$$A_2^\Omega(T, \mu) = A_{2,\text{FOPT}}^\Omega(T, \mu), \quad (17)$$

where

$$A_{2,\text{FOPT}}^\Omega(T, \mu) = \frac{(A_4^\Omega(T, \mu))^2}{4A_6^\Omega(T, \mu)} \quad (18)$$

Fig. 1 shows a schematic example of m dependence of $\Omega(T, \mu, h|m)$ at zero and finite magnetic field, see Eq. (1), when coefficient A_2^Ω is increases through $A_{2,\text{FOPT}}^\Omega$ value. One can see that at $h = 0$ global minimum position of m dependence of $\Omega(T, \mu, h|m)$ changes from $m = m_{\text{FM}}$ to $m = m_{\text{PM}}$ as $A_2^\Omega(T, \mu)$ becomes larger than $A_{2,\text{FOPT}}^\Omega(T, \mu)$. At $A_2^\Omega(T, \mu) > (4/3)A_{2,\text{FOPT}}^\Omega(T, \mu)$ local FM minimum disappears.

Let $m_{\text{FM}}^2, A_4^\Omega \rightarrow 0$ at FOPT line, so from Eq. (8) $A_2^\Omega \rightarrow 0$ and we arrive at *tricritical* point ($T = T_0^*, \mu = \mu^*$) for which $A_2^\Omega(T, \mu) = A_4^\Omega(T, \mu) = 0$. The continuation of FOPT line corresponding to equation $A_2^\Omega(T, \mu) = 0$ in $A_4^\Omega(T, \mu) > 0$ region yields SOPT line. Thereby, at tricritical point phase transition changes its order.

Using the Eqs. (17) and (8), we simplify the expression (9) for μ -fixed FM phase magnetic susceptibility

$$\bar{\chi}_{\text{FM}} = \frac{1}{8A_2^\Omega} > 0, \quad (19)$$

which is essentially positive in case of FOPT. Obtained results are applicable for both itinerant and localized (with replacements $\mu \rightarrow n$ and $\Omega \rightarrow F$) systems undergoing FOPT.

Finally, we should obtain the dependence of chemical potential $\mu = \mu_{\text{PS}}(T, h)$ to keep the system in the PS regime at finite h . The condition that the system remains in PS region when the magnetic field is applied is given by Eq. (16). Differentiating Eq. (16) with respect to h and taking into account the relation $\partial\Omega/\partial m = 0$ at $m = m_{\text{PM,FM}}$, we get

$$\begin{aligned} \frac{\partial\Omega}{\partial h}(T, \mu_{\text{PS}}(T, h), h|m_{\text{PM}}) + \frac{\partial\Omega}{\partial\mu}(T, \mu_{\text{PS}}(T, h), h|m_{\text{PM}}) \left(\frac{d\mu}{dh}\right)_{\text{PS}} \\ = \frac{\partial\Omega}{\partial h}(T, \mu_{\text{PS}}(T, h), h|m_{\text{FM}}) + \frac{\partial\Omega}{\partial\mu}(T, \mu_{\text{PS}}(T, h), h|m_{\text{FM}}) \left(\frac{d\mu}{dh}\right)_{\text{PS}}. \end{aligned} \quad (20)$$

We obtain an analogue of Clausius–Clapeyron relation determining the chemical potential derivative in Eq. (4) in the PS state as

$$\eta_{\text{PS}} \equiv \left(\frac{d\mu}{dh}\right)_{\text{PS}, h=0} = -\frac{m_{\text{FM}} - m_{\text{PM}}}{n_{\text{FM}} - n_{\text{PM}}}, \quad (21)$$

instead of η_n for single-phase case, see Eq. (14). Substituting the Eq. (1) into the last equation one obtains

$$\eta_{\text{PS}} = (1/m_{\text{FM}})(\dot{A}_2^\Omega + \dot{A}_4^\Omega m_{\text{FM}}^2 + \dot{A}_6^\Omega m_{\text{FM}}^4)^{-1}. \quad (22)$$

We have common $\eta = \eta_{\text{PS}}$ for both phases involved in PS differing by m value only. Then, using the equation of state (2), we get phase susceptibility

$$\chi_\Phi^{\text{PS}} = \bar{\chi}_\Phi \left(1 - \eta_{\text{PS}} \left(\frac{\partial f}{\partial \mu} \right)_\Phi \right). \quad (23)$$

So, we get directly

$$\chi_{\text{PM}}^{\text{PS}} = \bar{\chi}_{\text{PM}}, \quad (24)$$

$$\chi_{\text{FM}}^{\text{PS}} = -\bar{\chi}_{\text{FM}} \left(1 + \frac{2m_{\text{FM}}^2(\dot{A}_4^\Omega + 2\dot{A}_6^\Omega m_{\text{FM}}^2)}{\dot{A}_2^\Omega + \dot{A}_4^\Omega m_{\text{FM}}^2 + \dot{A}_6^\Omega m_{\text{FM}}^4} \right). \quad (25)$$

If m_{FM} is small (the vicinity of tricritical point) then the second term in brackets can be neglected and one get in the leading order with respect to m

$$\chi_{\text{FM}}^{\text{PS}} \simeq -\frac{1}{8A_2^\Omega} < 0. \quad (26)$$

One can see that in the vicinity of tricritical point $\chi_{\text{FM}}^{\text{PS}}$ is essentially negative (inverse sign with respect to Eq. (19)) and equal by absolute value to $\bar{\chi}_{\text{FM}}$ from Eq. (19).

Above we discussed magnetic susceptibilities of PM and FM phases involved in PS. We have shown that these two phases behave differently under the change of the magnetic field. There is significant contribution to magnetic susceptibility of FM phase involved in PS state that comes from a change in chemical potential as a function of the magnetic field (see Eqs. (21) and (23)), while for PM phase there is no such contribution since $(\partial f/\partial \mu)_{\text{PM}} = 0$. Let us stress here that total response for a system in the PS state should be obtained as a phase weighted average (see details in the model example below). To our knowledge this result is new, although some similar results (for example, a similar expression to Eq. (21) was obtained earlier for the alloys theory⁶⁶ for another problem).

C. Entropy calculation

We are mainly interested in the calculation of $(\Delta S)_{\text{env}}$ which is dependent on the physical environment (we mark this by the index “env”, (i) “env” = “n” and (ii) “env” = “PS”)

$$(\Delta S)_{\text{env}} = \int_0^h dh' \left(\frac{dS(h')}{dh'} \right)_{\text{env}}, \quad (27)$$

thus the sign of $(\Delta S)_{\text{env}}$ is defined by the sign of $(dS/dh)_{\text{env}}$ at small enough magnetic field.

By looking at the entropy definition $S = -\partial\Omega(T, \mu|m)/\partial T = S(T, \mu|m)$ one can see that S does not depend on magnetic field h explicitly, but only through chemical potential μ and magnetization m . So we have

$$\left(\frac{dS}{dh}\right)_{\text{env}} = \frac{\partial S}{\partial m}\chi_{\text{env}} + \frac{\partial S}{\partial \mu}\eta_{\text{env}}, \quad (28)$$

where η_{env} is determined by (5).

Now we discuss and compare the computation of the $(dS/dh)_{\text{env}}$ in both single-phase (i) and phase-separated (ii) cases. For the case (i) one gets

$$\left(\frac{\partial S}{\partial h}\right)_n = \chi_n \left(\frac{dS}{dm}\right)_n, \quad (29)$$

where

$$\left(\frac{\partial S}{\partial m}\right)_n = \left(\frac{\partial S}{\partial m} - \frac{\partial S}{\partial \mu} \frac{\partial \mathbf{n}/\partial m}{\partial \mathbf{n}/\partial \mu}\right), \quad (30)$$

with χ_n defined by Eq. (15).

Consider how the presence of PS and the negative sign of the magnetic response can affect the change in entropy when the magnetic field is applied. Let $S_\Phi(T, h) = S(T, \mu_{\text{PS}}(T, m_\Phi, h)|m_\Phi)$ be the entropy of phase Φ involved in PS.

From Eq. (28) one gets the entropy change derivative for the case (ii) for the phase Φ involved in PS

$$\left(\frac{dS_\Phi}{dh}\right)_{\text{PS}, \Phi} = \frac{\partial S}{\partial m}\chi_\Phi^{\text{PS}} + \frac{\partial S}{\partial \mu}\eta_{\text{PS}}, \quad (31)$$

where η_{PS} is determined by Eq. (21). Here it is taken into account that when the magnetic field is applied, not only the magnetization of the ferromagnetic phase m changes, but also μ . In the vicinity of tricritical point one can expect that the first (χ) term dominates over the second (η) term. Thus, we have

$$\left(\frac{dS_\Phi}{dh}\right)_{\text{PS}} = \frac{\chi_{\text{PS}}}{\chi_n} \left(\left(\frac{dS}{dh}\right)_n + \frac{\partial S}{\partial \mu} \left(\frac{\chi_n}{\chi_{\text{PS}}}\eta_{\text{PS}} - \eta_n \right) \right). \quad (32)$$

Thus, we have the contributions to the infinitesimal entropy change in FM phase: the χ term is opposite to the usual sign due to the negative phase susceptibility and η term has an uncertain sign. Therefore one can expect that an inverse MCE occurs as a direct consequence of PS for the parameter region for which direct MCE occurs away of PS region:

$$\left(\frac{dS_{\text{FM}}}{dh}\right)_{\text{PS}} > 0. \quad (33)$$

We state that the participation of FM phase in PS substantially can generally change both magnetic and entropy response. Furthermore, PS presence can change direct MCE away of PS region to the inverse MCE. For the paramagnetic phase involved in PS, the phase susceptibility is positive (see Eq. (6)). Thus, in the phase-separated (mixed) state, the magnetic response of the paramagnetic and ferromagnetic phases are opposite in sign, which can lead to the fact that the ferromagnetic phase contributes an inverse sign to the isothermal change of the entropy ΔS when the magnetic field is applied.

III. ENTROPY CHANGE FOR A FIRST-ORDER FM-PM TRANSITION INDUCED BY GIANT AN HOVE SINGULARITY: THE CASE OF FCC LATTICE

In this Section we present an example of calculation of generalized Landau theory coefficients A_α^Ω (see previous Section) and the MCE isothermal change of the entropy $\Delta S(T)$ for the case of non-degenerate Hubbard model face-centered cubic lattice

$$\mathcal{H} = \sum_{ij\sigma} t_{ij} c_{i\sigma}^\dagger c_{j\sigma} + U \sum_i n_{i\uparrow} n_{i\downarrow} - h \sum_{i\sigma} \sigma n_{i\sigma}, \quad (34)$$

where t_{ij} is non-zero and equal to t (t'), when sites i and j are nearest (next nearest) neighbours, $h = \mu_B H$ with H being a magnetic field, $c_{i\sigma}^\dagger/c_{i\sigma}$ is a creation/annihilation electron operator and $n_{i\sigma} = c_{i\sigma}^\dagger c_{i\sigma}$ is an operator of number of electrons with spin projection $\sigma = \pm 1$ at the site i , U is matrix element of local Coulomb interaction.

To cast giant van Hove singularity at the band bottom, we consider the case $t' = -t/2$, so the density of states for bare electron spectrum $\epsilon_{\mathbf{k}}^{\text{fcc}} = (1/N) \sum_{ij} t_{ij} \exp[i\mathbf{k}(\mathbf{R}_i - \mathbf{R}_j)]$ can be written

$$\tilde{\rho}_{\text{fcc}}(\epsilon) = \frac{1}{t} \sqrt{\frac{2}{3 + \epsilon/t}} \rho_{\text{sc}} \left(\sqrt{2} \sqrt{3 + \epsilon/t} \right), \quad (35)$$

where $\rho_{\text{sc}}(\epsilon)$ is the density of state (DOS) of simple cubic lattice spectrum within nearest neighbour approximation with unit hopping integral $t_{\text{sc}} = 1^{67-69}$. This expression has giant (square-root) van Hove singularity at the band bottom, $\epsilon = -3t$. To simplify calculations we replace $\rho_{\text{sc}}(\epsilon)$ by infinite-dimensional DOS for hypercubic lattice (hc)

$$\rho_{\text{hc}}^\infty(\epsilon) = \frac{1}{\sqrt{12\pi}} \exp[-\epsilon^2/12] \quad (36)$$

with the same $(\epsilon_{\mathbf{k}}^{\text{sc}})^2$ averaged over Brillouin zone as analogous $(\epsilon_{\mathbf{k}}^{\text{hc}})^2$ in the case of lattice

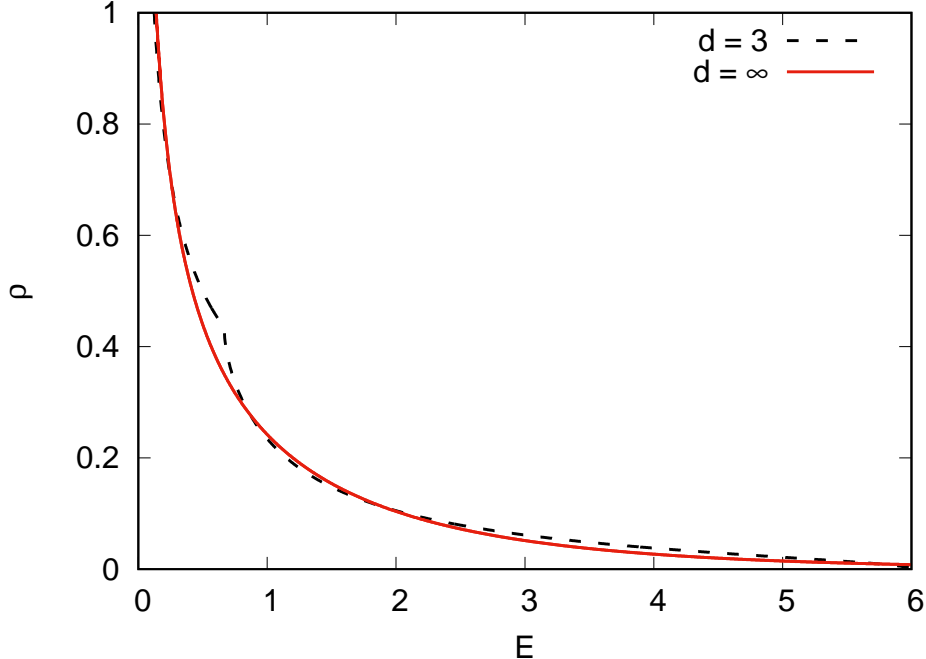


FIG. 2: Density of electronic states for a next nearest neighbor infinite-dimensional ($d = \infty$) and three-dimensional ($d = 3$) fcc lattice with $t' = -t/2$, see Eq. (37) and Refs. 68,69. The energy is calculated from the band bottom, $E = 1 + \epsilon/(3t)$.

dimension $d = \infty$. From Eqs. (35) and (36) we get the expression

$$\rho_{\text{fcc}}^{\infty}(E) = \frac{\exp(-E/2)}{\sqrt{2\pi E}}, \quad (37)$$

where dimensionless energy variable $E = 1 + \epsilon/(3t)$ is introduced, $\rho_{\text{fcc}}^{\infty}(E)dE = \tilde{\rho}_{\text{fcc}}^{\infty}(\epsilon)d\epsilon$, see Fig. 2. DOS for the case $d = \infty$ only weakly deviates from three-dimensional case in the vicinity of the band bottom, see Fig. 2. $\rho_{\text{fcc}}(\epsilon)$ only weakly deviates from $\rho_{\text{fcc}}^{\infty}(E)$ in the vicinity of band bottom. Below we take $3t$ as energy unit.

Further the Hubbard model is treated within the mean-field (Hartree-Fock, HFA) approximation under the assumption that we have ferromagnetic ordering induced by giant van Hove singularity at the band bottom. The application of HFA here is justified by the dominance of the crossed particle-hole electron-electron interaction channel^{70,71} with renormalized (screened) interaction parameter U . Due to the presence of a van Hove singularity in the vicinity of the Fermi level the Stoner criterion may be fulfilled with small enough U parameter.

A magnetization m (in units of μ_B) and a chemical potential μ are determined by following

HFA equations

$$n = \frac{1}{N} \sum_{\mathbf{k}\sigma} f_{\mu_0}(\varepsilon_{\mathbf{k}\sigma}), \quad (38)$$

and

$$m = \frac{1}{N} \sum_{\mathbf{k}\sigma} \sigma f_{\mu_0}(\varepsilon_{\mathbf{k}\sigma}), \quad (39)$$

where $f_{\mu}(\varepsilon_{\mathbf{k}\sigma})$ is the Fermi function with $\varepsilon_{\mathbf{k}\sigma} = \varepsilon_{\mathbf{k}}^{\text{fcc}} - \sigma(Um/2 + h)$ is HFA electronic spectrum. Within the HFA *effective* chemical potential $\mu_0 = \mu - Un/2$, subband spin splitting is $Um/2 + h$. At low T $\mu_0 \simeq E_f$.

At first, we discuss conventional approach allowing to describe the properties of paramagnetic and ferromagnetic phases for single-phase state. The corresponding thermodynamical potential is free energy⁴⁵

$$F_{\text{HFA}}(T, n, h|m) = \Omega_{\text{HFA}}(T, \mu, h|m) + \mu n, \quad (40)$$

where μ is determined by $\partial\Omega/\partial\mu = 0$ and HFA grand potential of a single-phase state reads

$$\begin{aligned} \Omega_{\text{HFA}}(T, \mu, h|m) = \Omega_0(T, \mu_0(T, n_{\text{HFA}}(T, \mu, m), m), Um/2 + h) \\ - (U/4)(n_{\text{HFA}}^2(T, \mu, m) - m^2), \end{aligned} \quad (41)$$

with grand potential of band (free) electrons

$$\Omega_0(T, \mu, h) = 2\mu - \frac{T}{N} \sum_{\mathbf{k}\sigma} \ln \left[2 \cosh \frac{\varepsilon_{\mathbf{k}}^{\text{fcc}} - \sigma h - \mu}{2T} \right], \quad (42)$$

where $n = n_{\text{HFA}}(T, \mu, m)$ is a solution of equation

$$\mu_0(T, n, m) = \mu - Un/2. \quad (43)$$

Here, auxiliary magnetic field (exchange splitting for *free* electronic subbands) h and charge field $\mu = \mu_0(T, n, m)$ are required to setup the magnetization and band filling values n, m .

The expansion of free energy defined by Eq. (40) is

$$F_{\text{HFA}}(T, n, h|m) = A_0^F(T, n) + A_2^F(T, n)m^2 + A_4^F(T, n)m^4 + A_6^F(T, n)m^4 - hm, \quad (44)$$

where $A_0^F(T, n)$ is a free energy at $m = 0$ and $h = 0$. Also,

$$A_2^F(T, n) = \frac{1}{4}(\Pi^{-1} - U), \quad (45)$$

$$A_4^F(T, n) = \frac{1}{64\Pi^5} \left(\Pi'^2 - \frac{1}{3}\Pi\Pi'' \right), \quad (46)$$

$$A_6^F(T, n) = \frac{1}{1536\Pi^7} \left(\frac{7\Pi'^2}{\Pi^2} \left(\Pi'^2 - \Pi\Pi'' \right) + \frac{2}{3}\Pi''^2 + \Pi'\Pi''' - \frac{1}{15}\Pi\Pi'''' \right), \quad (47)$$

where $\Pi = \Pi(T, E_F)$ with Fermi level corresponding to given band filling n , where

$$\Pi(T, E_F) = -\frac{1}{N} \sum_{\mathbf{k}} f'_{E_F}(\epsilon_{\mathbf{k}}^{\text{fcc}}) \quad (48)$$

is up to constant factor magnetic susceptibility in the paramagnetic phase. Prime above Π denotes E_F derivative.

The calculation of the dependence A_4^F on T and E_F using Eq. (46) allows to analyze the applicability of conventional approach. In the case $A_4^F > 0$ conventional Landau theory yields the phase transition line $A_2^F = 0$, separating FM region at $A_2^F < 0$, or equivalently

$$U\Pi(T, E_F) > 1, \quad (49)$$

from paramagnetic region at $A_2^F > 0$. In the case $T \rightarrow 0$ we get $\Pi(T, E_F) \rightarrow \rho(E_F)$ which transforms Eq. (49) into conventional Stoner criterion. Numerical calculation shows that A_4^F is negative in the small region in the vicinity of van Hove singularity position at small temperatures, see Fig. 3. We find that singular behaviour of $\rho(\epsilon)$ can change the sign of A_4^F and this makes the conventional Landau theory not applicable. In this situation it is necessary to consider accurately the possibility of FOPT FM-PM.

For itinerant electron system the FOPT results in phase separation which is convenient to investigate using $\Omega_{\text{HFA}}(T, \mu, h|m)$ instead of $F_{\text{HFA}}(T, n, h|m)$ using μ as main variable (see discussion in Refs.62–64). Such transition is accompanied not only by a jump of order parameter but also by jump of band filling.

Instead of expansion (44) one can use the expansion of Ω_{HFA} , see Eq. (41), cf. Sec. II, with explicit expressions for coefficients

$$A_2^\Omega(T, \mu) = \frac{1}{4}(\Pi^{-1} - U), \quad (50)$$

$$A_4^\Omega(T, \mu) = \frac{1}{192f\Pi^4}(3U\Pi'^2 - f\Pi''), \quad (51)$$

$$A_6^\Omega(T, \mu) = \frac{1}{720} \frac{1}{8f^3\Pi^7} \left(9(11f - 1)U^2\Pi'^4 - 3f(31f - 11)U\Pi''\Pi_0'^2 \right. \\ \left. + 2f^2(2f + 3)\Pi''^2 + 15f^2(f - 1)\Pi'''\Pi' - f^3\Pi''''\Pi \right), \quad (52)$$

where $f = 1 + U\Pi$, arguments T, μ of Π are omitted for brevity. Note that $A_2^\Omega(T, \mu) = A_2^F(T, n)$ with n and μ related by Eq. (38), but $A_4^\Omega \neq A_4^F$, $A_6^\Omega \neq A_6^F$. The derivation of Eqs. (50-52) will be published later⁷².

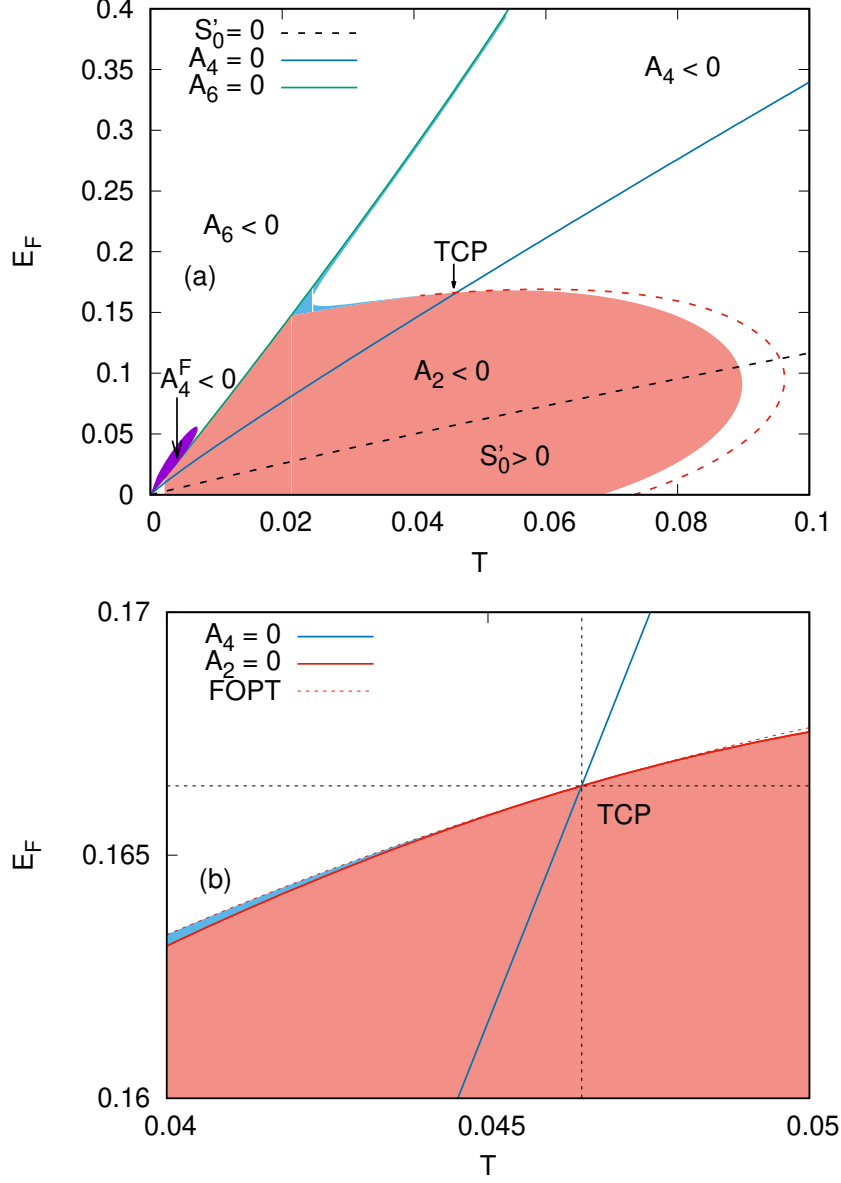


FIG. 3: (a) Phase diagram at $U = 1$ in terms T , E_F calculated within the generalized Landau theory, see Sec. II using coefficients A_2^Ω , A_4^Ω , A_6^Ω , see Eq. (50-52). $A_2^\Omega = 0$ corresponds to SOPT line when $A_4^\Omega, A_6^\Omega > 0$, FOPT line is set by $A_2^\Omega = A_{2,\text{FOPT}}^\Omega$. Dashed black line indicates line $S'_0(T, E_F) = 0$. Violet region indicates the region $A_4^F(T, E_F) < 0$ inside. Tricritical point (TCP) position is shown by an arrow. Red region indicates the region $A_2^\Omega < 0$, blue region indicates the region $0 < A_2^\Omega < A_{2,\text{FOPT}}^\Omega$, $A_4^\Omega < 0$. (b) The same as (a) in the vicinity of TCP.

The calculation of $A_\alpha^\Omega(T, \mu)$, $\alpha = 2, 4, 6$ using Eqs. (50-52) allows to calculate preliminary phase diagram within the generalized Landau theory, see Fig. 3. Accordingly to the discussion of Sec. II, in the case $A_6^\Omega > 0$ FM region corresponds to $A_2^\Omega < 0$ at $A_4^\Omega > 0$ and $A_2^\Omega < A_{2,\text{FOPT}}^\Omega$ for $A_4^\Omega < 0$. Otherwise PM phase is established. In the case $A_4^\Omega < 0$ the equation $A_2^\Omega = A_{2,\text{FOPT}}^\Omega$ yields FOPT line with corresponding PS region (see below); in the case $A_4^\Omega > 0$ the equation $A_2^\Omega = 0$ yields SOPT line. While using Ω expansion allows to make qualitative conclusions about phase diagram, it is very inconvenient for detailed calculations since necessary number of terms in the series to be hold is *a priori* unknown. To this end a better way is straightforward numerical minimization of Ω_{HFA} given by Eq. (41).

For definiteness we suppose that two possible phases are characterized by $n_{\text{FM}}(\mu, T, h)$, $m_{\text{FM}}(T, \mu, h)$ and $n_{\text{PM}}(T, \mu, h)$, $m_{\text{PM}}(T, \mu, h)$ and each of these sets of parameters provides the local minimum of Ω_{HFA} . In our consideration chemical potential μ governs the position of global minimum of Ω_{HFA} . So one can assume that there exists some critical value $\mu = \mu_{\text{PS}}$ so that $\Omega_{\text{HFA}}(\mu, T, h|m_{\text{FM}}) < \Omega_{\text{HFA}}(\mu, T, h|m_{\text{PM}})$ for $\mu < \mu_{\text{PS}}(T, h)$ and $\Omega_{\text{HFA}}(\mu, T|m_{\text{FM}}) > \Omega_{\text{HFA}}(\mu, T, h|m_{\text{FM}})$ for $\mu > \mu_{\text{PS}}(T, h)$ (arguments μ , T and h of $m_{\text{FM,PM}}$ are omitted for brevity). Thus, as μ increases, both m and n jump at $\mu = \mu_{\text{PS}}$, and a state with n satisfying $n_{\text{FM}} < n < n_{\text{PM}}$ corresponds to phase-separated state. The case of the second-order magnetic phase transition is reproduced within this scheme when $m_{\text{FM}} = m_{\text{PM}}$ (and therefore $n_{\text{FM}} = n_{\text{PM}}$): in this case phase separation is absent and treatments using F_{HFA} and Ω_{HFA} potentials are equivalent. An application of F_{HFA} -based scheme in the case $n_{\text{FM}} < n < n_{\text{PM}}$ results in thermodynamical unstable single-phase state. This is fully analogous to first-order transition water-vapour with pressure being analogous to $(-\mu)$ parameter, while H₂O density being analogous to n .

Using rather dense grid by μ and T variables allows to localize the position $\mu = \mu_{\text{PS}}$ where $\Omega_{\text{HFA}}(T, \mu, h|m_{\text{FM}}) = \Omega_{\text{HFA}}(T, \mu, h|m_{\text{PM}})$ for numerically calculated Ω_{HFA} . For given T , μ phase characteristics n_{FM} , m_{FM} and n_{PM} , m_{PM} are obtained by numerical solution of Eqs. (38-39). Fig. 4 presents the $T - n$ phase diagram at $U = 1.0$ including FM-PM phase separation region due to first-order transition at low temperatures for $n \simeq 0.6$ which provides the closeness of Fermi level to the band bottom (van Hove singularity). While in terms of $T - E_{\text{F}}$, see Fig. 3, FOPT line is very close to SOPT line, corresponding to FOPT line PS region is very wide. Phase boundaries are shown in two variants: in a zero and finite magnetic fields $h = 10^{-4}$. Curves denoting phase boundaries, $n = n_{\text{FM,PM}}(T, h)$, merge at $T = T^*(h)$ which

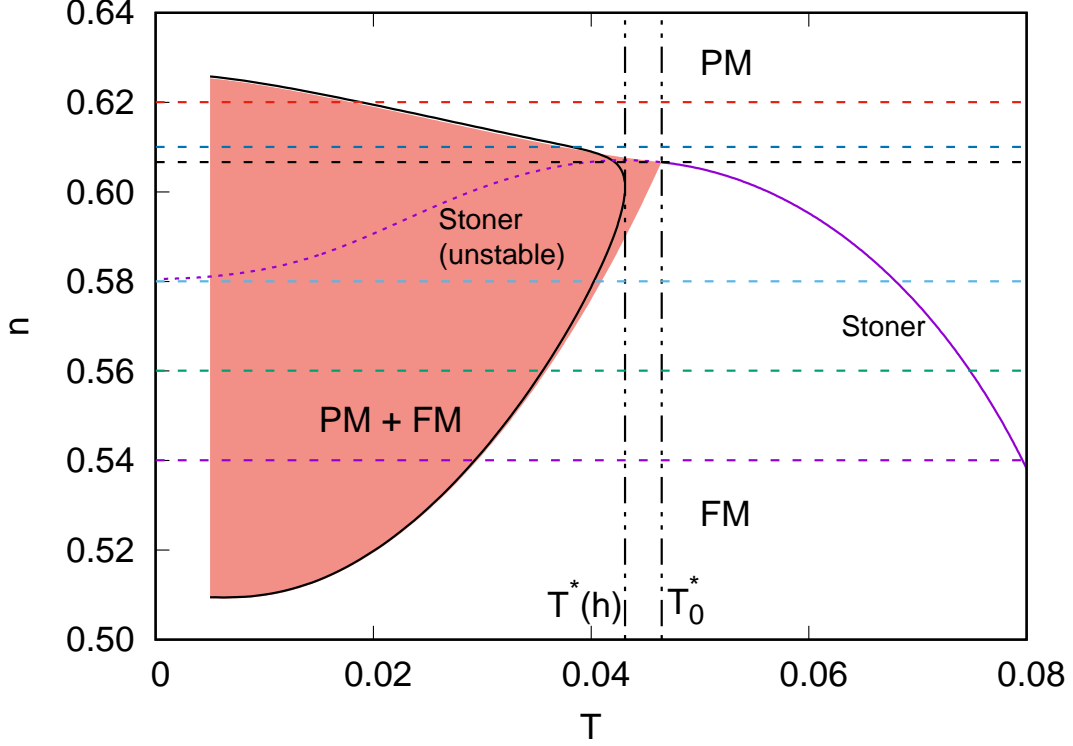


FIG. 4: $T - n$ phase diagram of the Hubbard model for an infinite-dimensional fcc lattice with $U = 1.0$. PS region FM + PM at $h = 0$ is filled by red color, black solid line indicates the corresponding PS boundary at finite h . Purple line is PM-FM phase boundary obtained from the Stoner criterion $U\Pi(T, E_F) = 1$. Its solid part corresponds to second-order phase FM-PM transition, whereas dotted part has no sense since it falls into the region of phase separation. The vertical dashed lines show the temperature boundaries of the phase separation in zero T_0^* (right) and finite $T^*(h)$ (left) magnetic field. Colors of horizontal dashed lines correspond to the values of n presented in Fig. 5.

corresponds to the tricritical point $(T^*(h), n^*(h))$, whose position depends on h . At $h = 0$ the position of tricritical point is $T_0^* \equiv T^*(h = 0) = 0.04645$, $n_0^* \equiv n^*(h = 0) = 0.6066$. At this point, a change in the order of phase transition occurs at $h = 0$: for $T > T_0^* \equiv T^*(h = 0)$, the phase transition is a second-order phase transition and the transition point is determined by the criterion $U\Pi(T, E_F) = 1$; for $T < T^*$ the curve determined by this criterion is inside the PS region and the criterion is inapplicable. We denote the temperature boundary of the PS region as $T_{\text{PS}}(n, h)$. From Fig. 4 it can be seen that when $n \simeq n^*$ the difference is $T_{\text{PS}}(n, h)$ from $T_{\text{PS}}(n, h = 0)$ can be significant.

Below we study $\Delta S(T)$ near temperature boundary $T_{\text{PS}}(n, h)$. Similar investigations of

$\Delta S(T)$ for Bethe lattice (second order phase transition) and square lattice (first order phase transition) are presented in Refs. 41–43. Here we calculate the entropy per site within the HFA as

$$S(\mu, T, h) = \sum_{\sigma} S_0(T, E_{F,\sigma}^{\text{HFA}}(\mu, n, m)), \quad (54)$$

where

$$E_{F,\sigma}^{\text{HFA}}(\mu, n, m) = \mu - Un/2 + \sigma(Um/2 + h) \quad (55)$$

being the effective Fermi level of σ spin subband for HFA solution for n and m , see Eqs. (38–39). An entropy per site and one spin subband for non-interacting electrons with spectrum $\epsilon_{\mathbf{k}}$ and Fermi level E_F is

$$S_0(T, E_F) = \frac{1}{N} \sum_{\mathbf{k}\sigma} \kappa \left(\frac{\epsilon_{\mathbf{k}} - E_F}{T} \right) \quad (56)$$

with auxiliary function

$$\kappa(x) = \ln [2 \cosh(x/2)] - (x/2) \tanh(x/2). \quad (57)$$

To calculate volume-averaged thermodynamical quantities such as m , S for the case of phase-separated state one needs to introduce the phase volume fractions $0 < x_{\text{FM}}, x_{\text{PM}} < 1$ for given n by the equation

$$n = x_{\text{FM}} n_{\text{FM}}(T, \mu_{\text{PS}}(T, h), h) + x_{\text{PM}} n_{\text{PM}}(T, \mu_{\text{PS}}(T, h), h), \quad (58)$$

together with $x_{\text{FM}} + x_{\text{PM}} = 1$. Then any extensive quantity is just a corresponding phase-weighted average. For example, total magnetization and entropy then are

$$m = x_{\text{FM}} m_{\text{FM}}(T, \mu_{\text{PS}}(T, h), h) + x_{\text{PM}} m_{\text{PM}}(T, \mu_{\text{PS}}(T, h), h), \quad (59)$$

$$S = x_{\text{FM}} S_{\text{FM}}(T, \mu_{\text{PS}}(T, h), h) + x_{\text{PM}} S_{\text{PM}}(T, \mu_{\text{PS}}(T, h), h), \quad (60)$$

where $m_{\text{FM,PM}}$ ($S_{\text{FM,PM}}$) is the phase magnetization (entropy) for both phases involved in PS.

Fig. 5 shows the temperature dependence of total m and ΔS (see Eqs. (59) and (60)) for the case $U = 1.0$ at various band fillings from the interval of PS existence $[0.50, 0.63]$ (these values are shown by horizontal lines on $T - n$ phase diagram, see Fig. 4). To illustrate the effect of PS on m and ΔS in Fig. 5 the temperature dependence of these quantities is also calculated within the assumption that the system is single-phase.

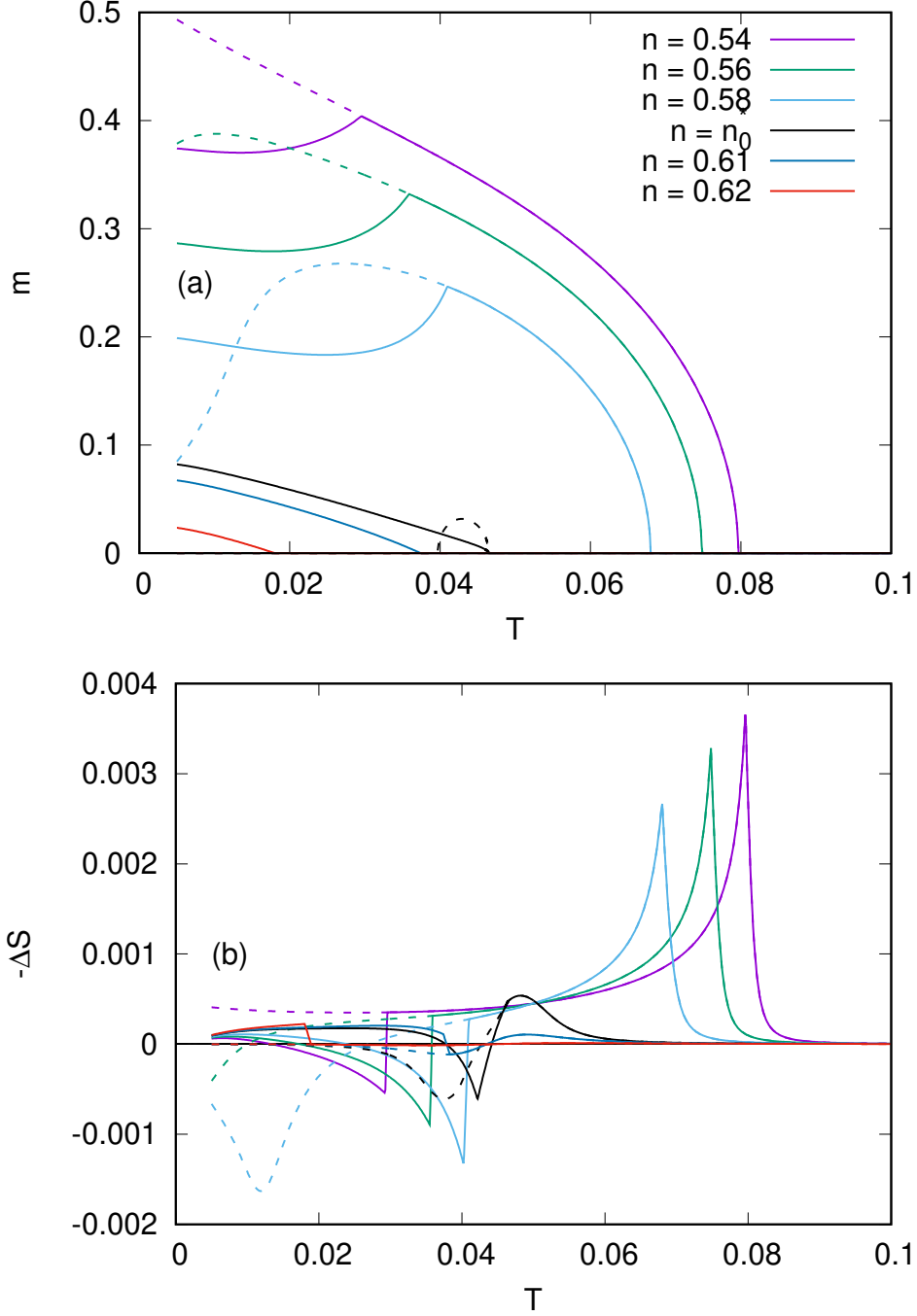


FIG. 5: Temperature dependence of (a) m , (b) ΔS for fillings in the vicinity of $n = n_0^* = 0.06066$ in the $[0.54, 0.62]$ filling interval. $U = 1.0, h = 10^{-4}$. Particular filling is shown by color, see the legend of Fig. 5. Dashed lines show the result of calculation by conventional way not taking into account PS possibility.

The temperature behavior of m and ΔS dramatically depends on n value. There is substantial effect of PS on m temperature dependence: at the $T = T_{\text{PS}}(n, 0)$ m dependence exhibit a valuable kink. The height of $m(T)$ kink decreases when n increases towards n^* . For the calculation not accounting PS formation, no kinks in $m(T)$ dependence is found, instead there is pyromagnetic behavior, which is an artifact of inconsistent treatment. When T approaches finite-field PS boundary $T_{\text{PS}}(n, h)$ with $n < n_0^*$ ΔS has a sharp peak and is positive (inverse MCE). With further increase in temperature in a narrow interval $[T_{\text{PS}}(n, h), T_{\text{PS}}(n, 0)]$ ΔS is almost linearly dependent on temperature, rapidly changing from positive peak to moderate negative value. With a further increase in T , a typical negative peak for the second-kind transition with $\Delta S < 0$ at $T = T_C$ takes place.

For $n > n_0^*$ there is a weak feature (kink) of the dependence ΔS associated with leaving the region of the phase separation, which height increases as n approaches n_0^* , but there is no second-order transition.

For $n \approx n_0^*$, the behavior of ΔS is the most interesting. The peculiarity is formed by an inverse MCE peak at the point $T = T^{\text{PS}}(n^*(h), h)$ and by a another direct MCE peak-like feature *not corresponding* to SOPT in the vicinity to $T = T_0^*$, between which there is a linear growth interval $[T^*(h), T_0^*]$ (for $n \neq n^*$ this temperature range has a smaller width).

The change of PS boundaries n_{FM} , n_{PM} under magnetic field switching is maximal at $T = T_0^*$. A remarkable consequence of this is a perspective of a control the sign and magnitude of Δ by changing the temperature in a narrow interval $[T^*(h), T^*]$, when $n \approx n_0^*$. When n significantly differs from n_0^* as the temperature increases, the system leaves PS area until a significant magnetic response is formed in the system.

Interestingly, the temperature dependencies $\Delta S(T)$ and $m(T)$ for small T are similar to that found for DyAl_2 ⁷³. Authors suppose that this anomaly is a consequence of an anisotropy and explains it within the Heisenberg model. The region of such dependence is limited by the temperature of the spin-flop transition. Here one can see an analogy with the results obtained, since the presence of two projections of magnetization along and perpendicular to the magnetic field in anisotropic systems is in a manner similar to the presence of two phases in phase-separated state of metallic systems.

Fig. 6 shows the temperature dependence of m and ΔS_{Φ} calculated separately for the phases Φ involved in PS in the case $U = 1.0$. Note that within the PS region, these quantities by definition do not depend on n , whereas n dependence of total ΔS orig-

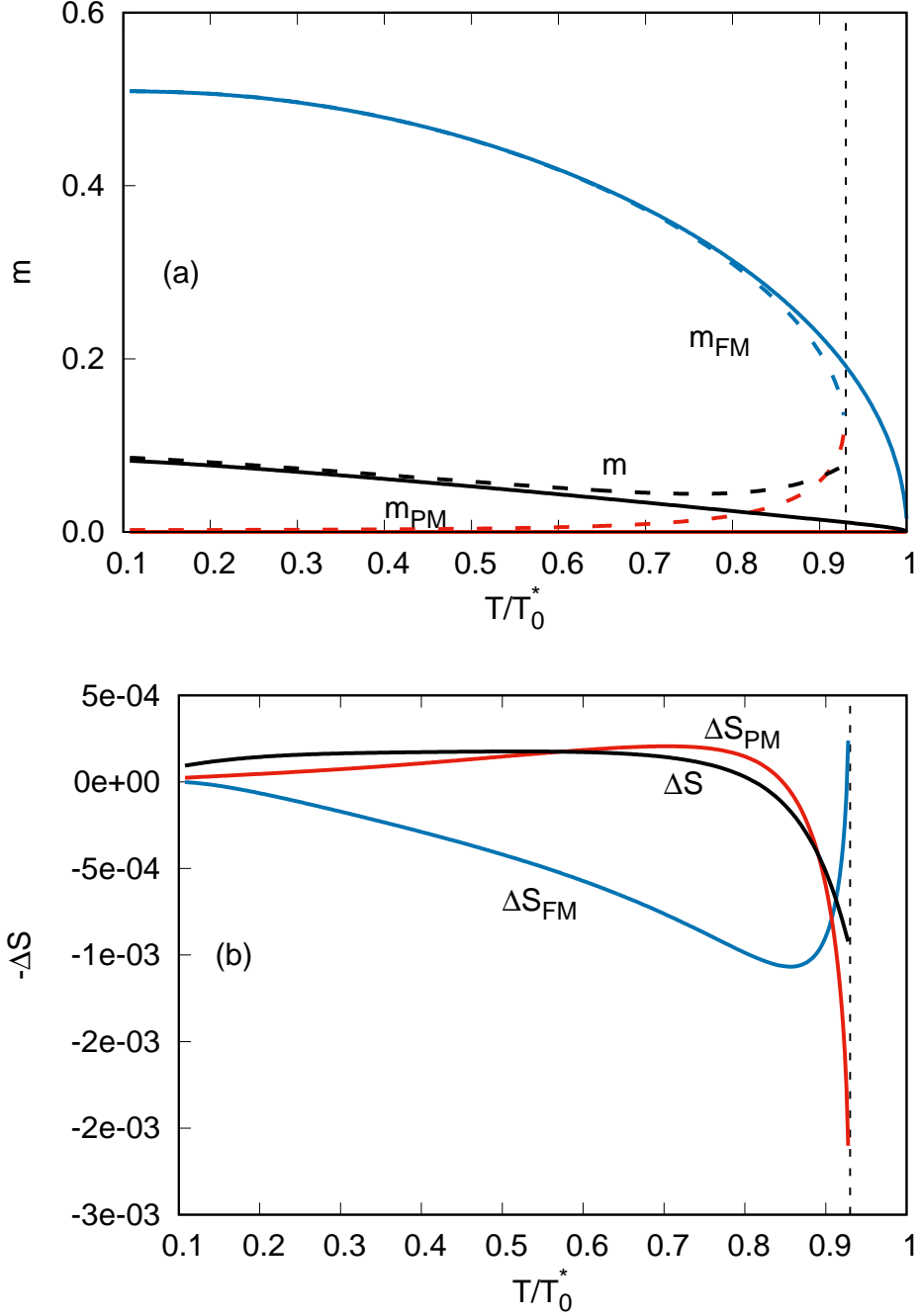


FIG. 6: (a) Temperature dependence of phase magnetization for ferromagnetic m_{FM} and paramagnetic m_{PM} phases involved in PS in zero magnetic field (solid lines) and finite magnetic field (dashed lines). (b) Temperature dependence of phase entropy change ΔS_{FM} and ΔS_{PM} . The temperature is taken in units of T_0^* . The vertical dashed line shows the position $T^*(h)$. The sample average value of ΔS and m for $n = n_0^*$ is shown for comparison. The parameters are the same as in Fig. 4.

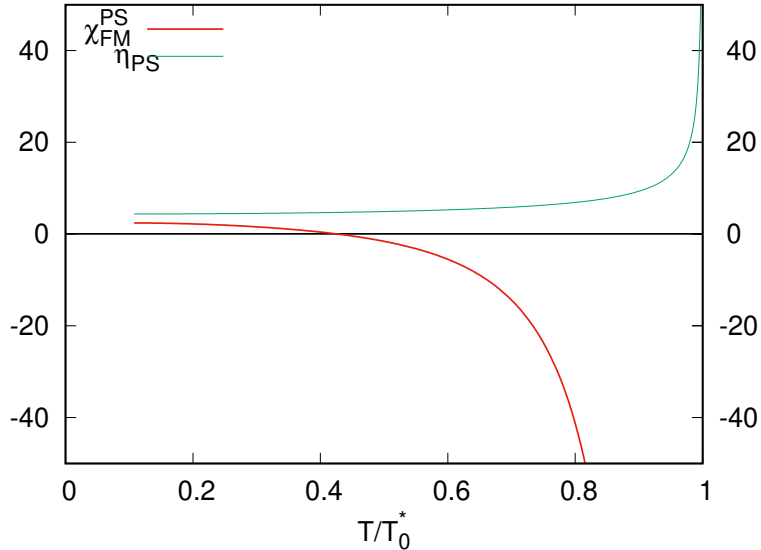


FIG. 7: Temperature dependence of phase FM susceptibility $\chi_{\text{FM}}^{\text{PS}}$ and η_{PS} at FOPT line. The temperature is taken in units of T_0^* . The parameters are the same as in Fig. 4.

inates from volume fraction n dependence only, see Eqs. (59-60). For the case $n = n_0^*$, T dependencies of total m and ΔS (averaged over the sample volume) are also shown. For the ferromagnetic phase, the magnetic response (susceptibility) to the magnetic field is negative at $T > 0.02 = 0.43T_0^*$ (see also Fig. 7 and derivation of this fact within the Landau theory in Sec. II) and we have inverse MCE effect, $\Delta S_{\text{FM}} > 0$, for almost all $T < T^*(h)$. For paramagnetic phase we have direct MCE effect $\Delta S_{\text{PM}} < 0$ up to $T < 0.0393 = 0.85T_0^*$. For the case $T > 0.85T_0^*$ we have rapid change of both phase ΔS_{FM} and ΔS_{PM} which is related with convergence m_{FM} and m_{PM} for phases involved in PS, see Eq. (6).

Effective Fermi level of both spin subbands $E_{\text{F},\sigma}^{\text{HFA}}$ at FOPT line, see Eq. (55), strongly depends on T . Fig. 8 shows $E_{\text{F},\sigma}^{\text{HFA}}$ in zero and finite for both phases involved in PS. One can see that effective Fermi level for \downarrow -subband $E_{\text{F},\downarrow}^{\text{HFA}}$ lies in the vicinity of van Hove singularity position $E = 0$.

A cause of inverse MCE for FM phase at FOPT line requires an explanation. In general, the reason for this fact is that when the magnetic field is applied, the chemical potential changes, adjusting n to into the phase separation region, cf. discussion in Sec. II. To reveal the origin of MCE sign dependence at FOPT line we calculate the magnetic field derivative

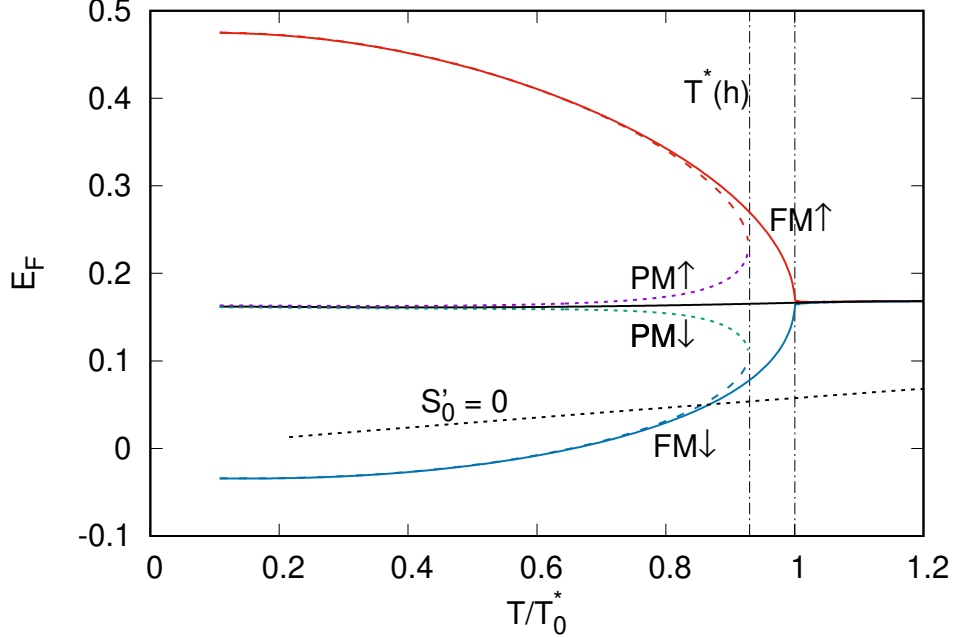


FIG. 8: Subband effective Fermi level $E_{F,\sigma}^{\text{HFA}}$ of FM and PM phase participating in PS in zero $h = 0$ (solid lines) and finite $h = 10^{-4}$ (dashed lines) magnetic field. Red (violet) lines correspond to FM (PM) phase $E_{F,\uparrow}^{\text{HFA}}$, blue (green) lines correspond to FM (PM) phase $E_{F,\downarrow}^{\text{HFA}}$. The parameters are the same as in Fig. 4. Black dotted line indicates the line $S'_0(T, E_F) = 0$, see Fig. 3. Vertical dot-dashed line indicates the temperature bound of PS region in finite $T^*(h)$ magnetic field. The temperature is taken in units of T_0^* . The parameters are the same as in Fig. 4.

of phase entropy for the phase Φ

$$\left(\frac{dS_\Phi}{dh}\right)_{\text{PS}} = \frac{1}{\Pi_\uparrow^\Phi + \Pi_\downarrow^\Phi + 2U\Pi_\uparrow^\Phi\Pi_\downarrow^\Phi} \sum_\sigma (\sigma(1 + U\Pi_\sigma^\Phi)\chi_\Phi^{\text{PS}} + 2\eta_{\text{PS}}\Pi_\sigma^\Phi) S'_0(T, E_{F,\sigma}^{\text{HFA}}(T, n_\Phi, m_\Phi)), \quad (61)$$

where η_{PS} is given by Eq. (21) and

$$\chi_\Phi^{\text{PS}} = \frac{\Pi_\uparrow^\Phi + \Pi_\downarrow^\Phi + 2U\Pi_\uparrow^\Phi\Pi_\downarrow^\Phi}{1 - U^2\Pi_\uparrow^\Phi\Pi_\downarrow^\Phi} + \frac{\Pi_\uparrow^\Phi - \Pi_\downarrow^\Phi}{1 - U^2\Pi_\uparrow^\Phi\Pi_\downarrow^\Phi} \eta_{\text{PS}}, \quad (62)$$

where $\Phi = \text{FM, PM}$ enumerates phases involved in PS and $\Pi_\sigma^\Phi = \Pi(T, E_{F,\sigma}^{\text{HFA}}(\mu, n_\Phi, m_\Phi))$. T dependencies of $(dS_\Phi/dh)_{\text{PS}}$ and $S'_0(T, E_{F,\sigma}^{\text{HFA}})$ for both spin projection in FM phase involved in PS are shown in Fig. 9. Subband contributions are proportional to $S'_0(E_{F,\sigma}^{\text{HFA}})$ which is shown in Fig. 9(b). One can see that S'_0 dominates for $\sigma = \downarrow$ and positive. The strong dependence of $(dS_{\text{FM}}/dh)_{\text{PS}}$ on T and the change in its sign are due to several facts: (i) $|S'_0(T, E_{F,\uparrow}^{\text{HFA}})| \ll S'_0(T, E_{F,\downarrow}^{\text{HFA}})$, (ii) the sign change of $S'_0(T, E_{F,\downarrow}^{\text{HFA}})$ at $T \approx 0.85T_0^*$, (iii)

the sign change of $\chi_{\text{PS}}^{\text{FM}}$ at $T \approx 0.02 = 0.43T_0^*$, see Fig. 7, cf. the discussion of negative susceptibility of FM phase in the vicinity of tricritical point.

At low temperature $\sigma = \downarrow$ contribution into $(dS_{\text{FM}}/dh)_{\text{PS}}$ dominates but χ - and η -terms have opposite signs and almost cancel each other. \downarrow χ -term is negative since in this T region both $S'_0(E_{\text{F},\downarrow}), \chi_{\text{FM}}^{\text{PS}} > 0$. At $T = 0.02 = 0.43T_0^*$ $\chi_{\text{FM}}^{\text{PS}}$ and, in turn, χ -term change their sign and both χ - and η -terms are positive which establishes inverse MCE for FM phase. η_{PS} holds its sign and the sign of η -term is fully determined by the sign of $S'_0(E_{\text{F},\downarrow})$. Further T increase results in dominating of χ -term over η -term. In the vicinity of T_0^* \downarrow -term χ and η -term as well as $S'_0(E_{\text{F},\downarrow}^{\text{HFA}})$ change their sign which results in sing change of $(dS_{\text{FM}}/dh)_{\text{PS}}$. The sign change of $S'_0(E_{\text{F}})$ is associated with giant van Hove singularity of the density of states at band bottom.

Now we see the reasons for the unusual behavior of ΔS in Fig. 4: the entropy of the paramagnetic phase decreases when the magnetic field is applied (excepting for T in a close vicinity of T_0^*), while the entropy of the ferromagnetic phase increases, it is directly related to a decrease in magnetization when applying the magnetic field (see Fig. 6) and impact of giant van Hove singularity of the density of states.

Thus, in the presence of a first-order phase transition sample-averaged inverse MCE effect can take place: when the magnetic field is applied, the FM-phase part of the sample is disordered and its entropy increases. There are two reasons for this: the presence of phase separation, which generally results in the sum of two phase contributions to ΔS , one of which is negative and the other is positive (the latter corresponds to inverse MCE); the second is the influence of giant van Hove singularity $\rho(\varepsilon)$, leading to the inverse sign ΔS already for the paramagnetic phase.

IV. CONCLUSIONS

This presentation models the first-order paramagnetic–ferromagnetic transition in the vicinity of the tricritical point for an itinerant system on fcc lattice for a small coupling constant which can simulate the formation of ferromagnetic order in itinerant compounds with giant van Hove singularity of the electron spectrum. While the Hartree-Fock approximation used is valid only qualitatively and it can be in principle replaced some better approximation, the above qualitative conclusions are valid for any itinerant system under-

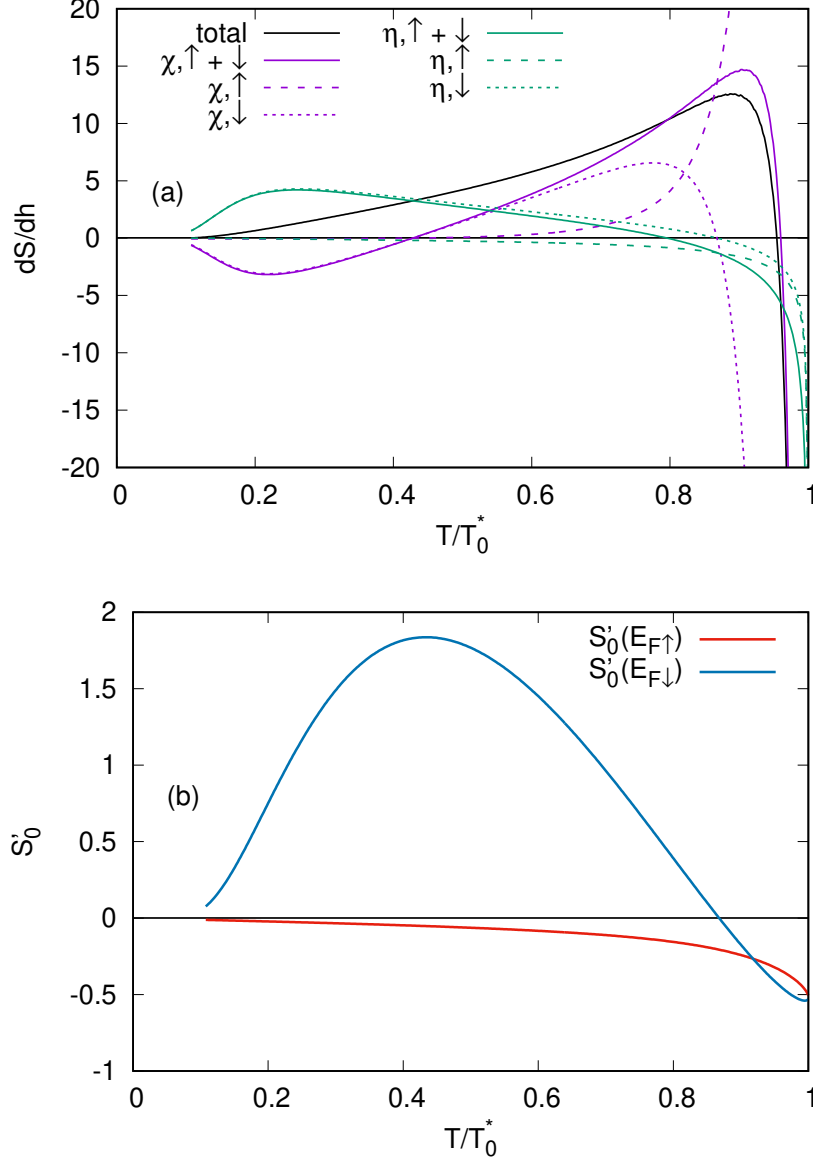


FIG. 9: Temperature dependence of properties for FM phase involved in PS. (a) The derivative dS_{FM}/dh see Eq. (61) (black line) and separate contributions into this: violet (green) lines indicate first χ -term (second η -term) in Eq. (61). Solid lines indicate sum of both spin projections contributions, dashed (dotted) line indicates spin up (down) projection. (b) $S'_0(E_{F,\sigma}^{\text{HFA}})$ for both spin projections. The temperature is taken in units of T_0^* . The parameters are the same as in Fig. 4.

going a first-order phase transition, which always leads to an unusual behavior of ΔS for the case when the electron filling lies in the corresponding filling interval. Independently on the approximation used FOPT results in phase separation which characteristics depend on approximation. The latter is thereby only quantitative effect. Note that the Coulomb

long-range energy not accounted for in the employed approximation cannot qualitatively change the results: as shown by the experiments of scanning tunnel microscopy⁷⁴, in such cases the system undergoes nanoscale phase separation (a specific implementation of the heterogeneity configuration can be fixed by the location of impurities and defects), which provides an energy minimum taking into account the energy of the Coulomb long-range action.

The role of van Hove singularity is manifold: (i) vHS is in general necessary origin of ferromagnetic ordering in itinerant electron systems, (ii) vHS results in first-order phase transition between paramagnetic and ferromagnetic phases with the corresponding phase separation, (iii) non-standard electronic properties caused by vHS result in turn inverse entropy response on the application of magnetic field.

It is shown that the magnetocalorical effect in metallic systems undergoing a first-order phase transition to the ferromagnetic state can have significant features due to the sample splitting into two phases having different values of band filling. To observe this effect, it is sufficient only to provide the special behavior of the density of states, no additional interactions should be considered. In particular, it was found that the contribution to ΔS from the ferromagnetic phase in the low-temperature region has an inverse sign. With increasing temperature, this contribution has pronounced peak at the temperature of the leaving PS region in a finite field and has a strong almost linear dependence inside the PS region in zero magnetic field and away PS PS region in finite magnetic field. This feature can find technical application in devices based on the control of the ΔS sign by changing the temperature or other parameters.

Perfect relation between nearest and next-nearest neighbour hopping producing giant van Hove singularity appears to be not absolutely necessary. Earlier investigations on the problem yields that some deviations from this relation results in the replacement of divergence of DOS by a wide plateau with high value of $\rho(\epsilon)$ ^{69,71,75,76}. This does not completely breaks anomalous thermodynamical properties which allows to expect the PS existence and inverse MCE in this case.

The description of MCE within a novel generalized Landau theory can acquire perspective extensions taking into account additional interactions like magnetoelastic coupling⁷⁷ and spin-fluctuations⁷⁸ etc.

V. ACKNOWLEDGMENTS

We are grateful to V. Yu. Irkhin, A. N. Ignatenko, N. S. Pavlov for fruitful discussions. The theoretical studies in Section 2 is supported by the state assignment of the Ministry of Science and Higher Education of the Russian Federation (theme “Quant” No. 122021000038-7) for development of generalized Landau functional approach. The theoretical studies in Section 3 are in part supported by the Russian Science Foundation (Project No. 24-43-00156) for entropy calculations within Hartree-Fock approximation for the Hubbard model.

-
- ¹ V. Franco, J. Blázquez, B. Ingale, and A. Conde, *Annual Review of Materials Research* **42**, 305 (2012).
- ² L.-W. Li, *Chinese Physics B* **25**, 037502 (2016), URL <https://dx.doi.org/10.1088/1674-1056/25/3/037502>.
- ³ V. Franco, J. Blázquez, J. Ipus, J. Law, L. Moreno-Ramírez, and A. Conde, *Progress in Materials Science* **93**, 112 (2018), ISSN 0079-6425, URL <https://www.sciencedirect.com/science/article/pii/S0079642517301299>.
- ⁴ A. Tishin and Y. Spichkin, *International Journal of Refrigeration* **37**, 223 (2014), ISSN 0140-7007, new Developments in Magnetic Refrigeration, URL <https://www.sciencedirect.com/science/article/pii/S0140700713002466>.
- ⁵ A. Tishin, Y. Spichkin, V. Zverev, and P. Egolf, *International Journal of Refrigeration* **68**, 177 (2016), ISSN 0140-7007, URL <https://www.sciencedirect.com/science/article/pii/S0140700716300615>.
- ⁶ N. de Oliveira and P. von Ranke, *Physics Reports* **489**, 89 (2010), ISSN 0370-1573, URL <https://www.sciencedirect.com/science/article/pii/S0370157309002907>.
- ⁷ H. Fu, Z. Ma, X. J. Zhang, D. H. Wang, B. H. Teng, and E. Agurgo Balfour, *Applied Physics Letters* **104**, 072401 (2014), ISSN 0003-6951, https://pubs.aip.org/aip/apl/article-pdf/doi/10.1063/1.4865554/13682208/072401-1_online.pdf, URL <https://doi.org/10.1063/1.4865554>.
- ⁸ E. Agurgo Balfour, Z. Ma, H. Fu, R. L. Hadimani, D. C. Jiles, L. Wang, Y. Luo, and S. F. Wang, *Journal of Applied Physics*

- 118**, 123903 (2015), ISSN 0021-8979, https://pubs.aip.org/aip/jap/article-pdf/doi/10.1063/1.4931765/15168795/123903_1_online.pdf, URL <https://doi.org/10.1063/1.4931765>.
- ⁹ G. L. Liu, D. Q. Zhao, H. Y. Bai, W. H. Wang, and M. X. Pan, *Journal of Physics D: Applied Physics* **49**, 055004 (2016), URL <https://dx.doi.org/10.1088/0022-3727/49/5/055004>.
- ¹⁰ Q. Zheng, L. Zhang, and J. Du, *Journal of Physics D: Applied Physics* **50**, 355601 (2017), URL <https://dx.doi.org/10.1088/1361-6463/aa7a8f>.
- ¹¹ X. Zhong, X. Shen, H. Mo, D. Jiao, Z. Liu, W. Qiu, H. Zhang, and R. Ramanujan, *Materials Today Communications* **14**, 22 (2018), ISSN 2352-4928, URL <https://www.sciencedirect.com/science/article/pii/S2352492817303239>.
- ¹² V. K. Pecharsky and K. A. Gschneidner, Jr., *Phys. Rev. Lett.* **78**, 4494 (1997), URL <https://link.aps.org/doi/10.1103/PhysRevLett.78.4494>.
- ¹³ H. Wada, K. Taniguchi, and Y. Tanabe, *MATERIALS TRANSACTIONS* **43**, 73 (2002).
- ¹⁴ O. Tegus, E. Brück, K. H. J. Buschow, and F. R. de Boer, *Nature* **415**, 150 (2002).
- ¹⁵ A. Fujita, K. Fukamichi, J.-T. Wang, and Y. Kawazoe, *Phys. Rev. B* **68**, 104431 (2003), URL <https://link.aps.org/doi/10.1103/PhysRevB.68.104431>.
- ¹⁶ V. Franco, J. Y. Law, A. Conde, V. Brabander, D. Y. Karpenkov, I. Radulov, K. Skokov, and O. Gutfleisch, *Journal of Physics D: Applied Physics* **50**, 414004 (2017), URL <https://dx.doi.org/10.1088/1361-6463/aa8792>.
- ¹⁷ H. Yamada and T. Goto, *Phys. Rev. B* **68**, 184417 (2003), URL <https://link.aps.org/doi/10.1103/PhysRevB.68.184417>.
- ¹⁸ X. Zhang, B. Zhang, S. Yu, Z. Liu, W. Xu, G. Liu, J. Chen, Z. Cao, and G. Wu, *Phys. Rev. B* **76**, 132403 (2007), URL <https://link.aps.org/doi/10.1103/PhysRevB.76.132403>.
- ¹⁹ T. Krenke, E. Duman, M. Acet, E. F. Wassermann, X. Moya, L. Mañosa, and A. Planes, *Nature Materials* **4**, 450 (2005), cond-mat/0505652.
- ²⁰ B. Wang and Y. Liu, *Metals* **3**, 69 (2013), ISSN 2075-4701, URL <https://www.mdpi.com/2075-4701/3/1/69>.
- ²¹ M. Hsini, S. Hcini, and S. Zemni, *Journal of Magnetism and Magnetic Materials* **466**, 368 (2018), ISSN 0304-8853, URL <https://www.sciencedirect.com/science/article/pii/S030488531830547X>.
- ²² L. Caron, Z. Ou, T. Nguyen, D. Cam Thanh, O. Tegus, and

- E. Brück, *Journal of Magnetism and Magnetic Materials* **321**, 3559 (2009), ISSN 0304-8853, current Perspectives: Magnetocaloric Materials, URL <https://www.sciencedirect.com/science/article/pii/S0304885309006787>.
- ²³ E. Restrepo-Parra, L. Ramos-Rivera, and J. Londoño-Navarro, *Journal of Magnetism and Magnetic Materials* **351**, 65 (2014), ISSN 0304-8853, URL <https://www.sciencedirect.com/science/article/pii/S0304885313006616>.
- ²⁴ P. J. von Ranke, V. K. Pecharsky, K. A. Gschneidner, and B. J. Korte, *Phys. Rev. B* **58**, 14436 (1998), URL <https://link.aps.org/doi/10.1103/PhysRevB.58.14436>.
- ²⁵ T. Samanta, I. Das, and S. Banerjee, *Applied Physics Letters* **91**, 152506 (2007), ISSN 0003-6951, https://pubs.aip.org/aip/apl/article-pdf/doi/10.1063/1.2798594/14382714/152506_1_online.pdf, URL <https://doi.org/10.1063/1.2798594>.
- ²⁶ K. G. Sandeman, R. Daou, S. Özcan, J. H. Durrell, N. D. Mathur, and D. J. Fray, *Phys. Rev. B* **74**, 224436 (2006), URL <https://link.aps.org/doi/10.1103/PhysRevB.74.224436>.
- ²⁷ J. Gschneidner, K. A., V. K. Pecharsky, and A. O. Tsokol, *Reports on Progress in Physics* **68**, 1479 (2005).
- ²⁸ G. J. Liu, J. R. Sun, J. Z. Wang, and B. G. Shen, *Applied Physics Letters* **89**, 222503 (2006), ISSN 0003-6951, https://pubs.aip.org/aip/apl/article-pdf/doi/10.1063/1.2397535/14367199/222503_1_online.pdf, URL <https://doi.org/10.1063/1.2397535>.
- ²⁹ M. H. Phan, M. B. Morales, N. S. Bingham, H. Srikanth, C. L. Zhang, and S. W. Cheong, *Phys. Rev. B* **81**, 094413 (2010), URL <https://link.aps.org/doi/10.1103/PhysRevB.81.094413>.
- ³⁰ M. Annaorazov, K. Asatryan, G. Myalikhulyev, S. Nikitin, A. Tishin, and A. Tyurin, *Cryogenics* **32**, 867 (1992), ISSN 0011-2275, URL <https://www.sciencedirect.com/science/article/pii/001122759290352B>.
- ³¹ R. R. Gimaev, A. A. Vaulin, A. F. Gubkin, and V. I. Zverev, *Physics of Metals and Metallography* **121**, 823–850 (2020).
- ³² M. Balli, D. Fruchart, and R. Zach, *Journal of Applied Physics* **115**, 203909 (2014), ISSN 0021-8979, https://pubs.aip.org/aip/jap/article-pdf/doi/10.1063/1.4880397/15138779/203909_1_online.pdf, URL <https://doi.org/10.1063/1.4880397>.

- ³³ D. Khedr, S. H. Aly, R. M. Shabara, and S. Yehia, *Journal of Magnetism and Magnetic Materials* **475**, 436 (2019), ISSN 0304-8853, URL <https://www.sciencedirect.com/science/article/pii/S0304885318320316>.
- ³⁴ P. Álvarez-Alonso, P. Gorria, J. A. Blanco, J. Sánchez-Marcos, G. J. Cuello, I. Puente-Orench, J. A. Rodríguez-Velamazán, G. Garbarino, I. de Pedro, J. R. Fernández, et al., *Phys. Rev. B* **86**, 184411 (2012), URL <https://link.aps.org/doi/10.1103/PhysRevB.86.184411>.
- ³⁵ P. J. von Ranke, I. G. de Oliveira, A. P. Guimarães, and X. A. da Silva, *Phys. Rev. B* **61**, 447 (2000), URL <https://link.aps.org/doi/10.1103/PhysRevB.61.447>.
- ³⁶ V. B. Naik, S. K. Barik, R. Mahendiran, and B. Raveau, *Applied Physics Letters* **98**, 112506 (2011), ISSN 0003-6951, https://pubs.aip.org/aip/apl/article-pdf/doi/10.1063/1.3567760/13219399/112506_1_online.pdf, URL <https://doi.org/10.1063/1.3567760>.
- ³⁷ R. dos Reis, L. da Silva, A. dos Santos, A. Medina, L. Cardoso, and F. Gandra, *Journal of Alloys and Compounds* **582**, 461 (2014), ISSN 0925-8388, URL <https://www.sciencedirect.com/science/article/pii/S0925838813018690>.
- ³⁸ H. Zhang, Y. J. Sun, L. H. Yang, E. Niu, H. S. Wang, F. X. Hu, J. R. Sun, and B. G. Shen, *Journal of Applied Physics* **115**, 063901 (2014), ISSN 0021-8979, https://pubs.aip.org/aip/jap/article-pdf/doi/10.1063/1.4865297/13379409/063901_1_online.pdf, URL <https://doi.org/10.1063/1.4865297>.
- ³⁹ D. Comtesse, M. E. Gruner, M. Ogura, V. V. Sokolovskiy, V. D. Buchelnikov, A. Grünebohm, R. Arróyave, N. Singh, T. Gottschall, O. Gutfleisch, et al., *Phys. Rev. B* **89**, 184403 (2014), URL <https://link.aps.org/doi/10.1103/PhysRevB.89.184403>.
- ⁴⁰ V. Sokolovskiy, M. Zagrebin, and V. D. Buchelnikov, *Journal of Magnetism and Magnetic Materials* **459**, 295 (2018), ISSN 0304-8853, the selected papers of Seventh Moscow International Symposium on Magnetism (MISM-2017), URL <https://www.sciencedirect.com/science/article/pii/S0304885317321522>.
- ⁴¹ P. A. Igoshev, E. E. Kokorina, and I. A. Nekrasov, *Physics of Metals and Metallography* **118**, 207–216 (2017), URL <https://link.springer.com/article/10.1134/S0031918X17030048>.
- ⁴² V. V. Ivchenko and P. A. Igoshev, *Phys. Rev. B* **104**, 024425 (2021), URL <https://link.aps.org/doi/10.1103/PhysRevB.104.024425>.

- ⁴³ P. A. Igoshev, L. N. Gramateeva, and A. V. Lukoyanov, *Phys. Chem. Chem. Phys.* **25**, 6995 (2023), URL <http://dx.doi.org/10.1039/D2CP05923A>.
- ⁴⁴ L. D. Landau and E. M. Lifshitz, *Statistical Physics: Volume 5*, vol. 5 (Elsevier, 2013).
- ⁴⁵ T. Moriya, *Spin fluctuations in itinerant electron magnetism*, vol. 56 (Springer Science & Business Media, 2012).
- ⁴⁶ K. K. Murata and S. Doniach, *Phys. Rev. Lett.* **29**, 285 (1972), URL <https://link.aps.org/doi/10.1103/PhysRevLett.29.285>.
- ⁴⁷ T. Moriya and A. Kawabata, *Journal of the Physical Society of Japan* **34**, 639 (1973), <https://doi.org/10.1143/JPSJ.34.639>, URL <https://doi.org/10.1143/JPSJ.34.639>.
- ⁴⁸ T. Moriya and A. Kawabata, *Journal of the Physical Society of Japan* **35**, 669 (1973), <https://doi.org/10.1143/JPSJ.35.669>, URL <https://doi.org/10.1143/JPSJ.35.669>.
- ⁴⁹ N. A. de Oliveira, *The European Physical Journal B - Condensed Matter and Complex Systems* **40**, 259 (2004), ISSN 1434-6036, URL <https://doi.org/10.1140/epjb/e2004-00267-9>.
- ⁵⁰ L. de Medeiros, N. de Oliveira, P. von Ranke, and A. Troper, *Physica A: Statistical Mechanics and its Applications* **392**, 1355 (2013), ISSN 0378-4371, URL <https://www.sciencedirect.com/science/article/pii/S0378437112010114>.
- ⁵¹ N. A. de Oliveira and P. J. von Ranke, *Journal of Physics: Condensed Matter* **17**, 3325 (2005), URL <https://dx.doi.org/10.1088/0953-8984/17/21/025>.
- ⁵² D. Bloch, D. M. Edwards, M. Shimizu, and J. Voiron, *Journal of Physics F: Metal Physics* **5**, 1217 (1975), URL <https://dx.doi.org/10.1088/0305-4608/5/6/022>.
- ⁵³ N. H. Duc, D. Givord, C. Lacroix, and C. Pinettes, *Europhysics Letters* **20**, 47 (1992), URL <https://dx.doi.org/10.1209/0295-5075/20/1/009>.
- ⁵⁴ M. Balli, D. Fruchart, D. Gignoux, and R. Zach, *Applied Physics Letters* **95**, 072509 (2009), ISSN 0003-6951, https://pubs.aip.org/aip/apl/article-pdf/doi/10.1063/1.3194144/14106384/072509_1_online.pdf, URL <https://doi.org/10.1063/1.3194144>.
- ⁵⁵ V. Pecharsky, K. Gschneidner, Y. Mudryk, and D. Paudyal, *Journal of Magnetism and Magnetic Materials* **321**, 3541 (2009), ISSN 0304-8853, current Perspectives: Magnetocaloric Materials, URL <https://www.sciencedirect.com/science/article/pii/S0304885308002862>.
- ⁵⁶ K. Xu, Z. Li, Y.-L. Zhang, and C. Jing, *Physics Letters A* **379**, 3149 (2015), ISSN 0375-9601, URL <https://www.sciencedirect.com/science/article/pii/S0375960115009019>.

- ⁵⁷ F. Casanova, X. Batlle, A. Labarta, J. Marcos, L. Mañosa, and A. Planes, *Journal of Applied Physics* **93**, 8313 (2003), ISSN 0021-8979, https://pubs.aip.org/aip/jap/article-pdf/93/10/8313/18931353/8313_1_online.pdf, URL <https://doi.org/10.1063/1.1556274>.
- ⁵⁸ L. Jia, G. J. Liu, J. R. Sun, H. W. Zhang, F. X. Hu, C. Dong, G. H. Rao, and B. G. Shen, *Journal of Applied Physics* **100**, 123904 (2006), ISSN 0021-8979, https://pubs.aip.org/aip/jap/article-pdf/doi/10.1063/1.2404468/13571284/123904_1_online.pdf, URL <https://doi.org/10.1063/1.2404468>.
- ⁵⁹ K. Matsumoto, T. Okano, T. Kouen, S. Abe, T. Numazawa, K. Kamiya, and S. Nimori, *IEEE Transactions on Applied Superconductivity* **14**, 1738 (2004).
- ⁶⁰ V. K. Pecharsky and K. A. Gschneidner, Jr., *Phys. Rev. Lett.* **78**, 4494 (1997), URL <https://link.aps.org/doi/10.1103/PhysRevLett.78.4494>.
- ⁶¹ G. J. Liu, J. R. Sun, J. Shen, B. Gao, H. W. Zhang, F. X. Hu, and B. G. Shen, *Applied Physics Letters* **90**, 032507 (2007), ISSN 0003-6951, https://pubs.aip.org/aip/apl/article-pdf/doi/10.1063/1.2425033/13184831/032507_1_online.pdf, URL <https://doi.org/10.1063/1.2425033>.
- ⁶² P. Igoshev, A. Katanin, H. Yamase, and V. Y. Irkhin, *Journal of Magnetism and Magnetic Materials* **321**, 899 (2009), ISSN 0304-8853, proceedings of the Forth Moscow International Symposium on Magnetism, URL <https://www.sciencedirect.com/science/article/pii/S0304885308012377>.
- ⁶³ P. A. Igoshev, M. A. Timirgazin, A. A. Katanin, A. K. Arzhnikov, and V. Y. Irkhin, *Phys. Rev. B* **81**, 094407 (2010), URL <https://link.aps.org/doi/10.1103/PhysRevB.81.094407>.
- ⁶⁴ P. A. Igoshev, M. A. Timirgazin, V. F. Gilmudinov, A. K. Arzhnikov, and V. Y. Irkhin, *Journal of Physics: Condensed Matter* **27**, 446002 (2015), URL <https://dx.doi.org/10.1088/0953-8984/27/44/446002>.
- ⁶⁵ P. A. Igoshev, *Physics of Metals and Metallography* **124**, 1112 (2023), ISSN 1555-6190, URL <https://doi.org/10.1134/S0031918X23602147>.
- ⁶⁶ M. Krivoglaz and V. Sadovskii, *Fiz. Met. Metalloved* **18**, 502 (1964).
- ⁶⁷ D. Vollhardt, N. Blümer, K. Held, M. Kollar, J. Schlipf, and M. Ulmke, *Zeitschrift für Physik B Condensed Matter* **103**, 283 (1996), ISSN 1431-584X, URL <https://doi.org/10.1007/s002570050375>.
- ⁶⁸ M. Ulmke, *The European Physical Journal B - Condensed Matter and Complex Systems* **1**, 301

- (1998), ISSN 1434-6036, URL <https://doi.org/10.1007/s100510050186>.
- ⁶⁹ P. Igoshev and V. Irkhin, *Physics Letters A* **438**, 128107 (2022), ISSN 0375-9601, URL <https://www.sciencedirect.com/science/article/pii/S037596012200189X>.
- ⁷⁰ W. Metzner, M. Salmhofer, C. Honerkamp, V. Meden, and K. Schönhammer, *Rev. Mod. Phys.* **84**, 299 (2012), URL <https://link.aps.org/doi/10.1103/RevModPhys.84.299>.
- ⁷¹ P. A. Igoshev and A. A. Katanin, *Phys. Rev. B* **107**, 115105 (2023), URL <https://link.aps.org/doi/10.1103/PhysRevB.107.115105>.
- ⁷² P. Igoshev (2024).
- ⁷³ A. L. Lima, A. O. Tsokol, K. A. Gschneidner, V. K. Pecharsky, T. A. Lograsso, and D. L. Schlagel, *Phys. Rev. B* **72**, 024403 (2005), URL <https://link.aps.org/doi/10.1103/PhysRevB.72.024403>.
- ⁷⁴ I. Battisti, K. M. Bastiaans, V. Fedoseev, A. De La Torre, N. Iliopoulos, A. Tamai, E. C. Hunter, R. S. Perry, J. Zaanen, F. Baumberger, et al., *Nature physics* **13**, 21 (2017).
- ⁷⁵ P. A. Igoshev and V. Y. Irkhin, *Physics of Metals and Metallography* **120**, 1282 (2019), ISSN 1555-6190, URL <https://doi.org/10.1134/S0031918X19130088>.
- ⁷⁶ P. A. Igoshev and V. Y. Irkhin, *JETP Letters* **110**, 727 (2019), ISSN 1090-6487, URL <https://doi.org/10.1134/S0021364019230085>.
- ⁷⁷ S. M. Podgornykh and Y. V. Shcherbakova, *Phys. Rev. B* **73**, 184421 (2006), URL <https://link.aps.org/doi/10.1103/PhysRevB.73.184421>.
- ⁷⁸ P. A. Igoshev, A. A. Katanin, and V. Y. Irkhin, *Journal of Experimental and Theoretical Physics* **105**, 1043 (2007), ISSN 1090-6509, URL <https://doi.org/10.1134/S1063776107110167>.